BONE MORPHOGENETIC PROTEIN BINDING ENDOTHELIAL REGULATOR (BMPER) REGULATES VASCULAR INFLAMMATORY RESPONSES IN ENDOTHELIAL CELLS

Pamela P. Lockyer

A thesis submitted to the faculty at the University of North Carolina at Chapel Hill in partial fulfillment of the requirements for the degree of Master of Science in the Department of Pathology and Laboratory Medicine in the School of Medicine.

Chapel Hill
2017

Approved by:

Jonathan Homeister

Xinchun Pi

Joan Taylor

ABSTRACT

Pamela P. Lockyer: Bone Morphogenetic Protein Binding Endothelial Regulator (BMPER) Regulates Vascular Inflammatory Responses in Endothelial Cells
(Under the direction of Xinchun Pi)

Dysfunction of the vascular endothelium results in various cardiovascular, circulatory and blood diseases highlighting the importance of endothelial integrity. How BMPER mediates signaling events to regulate endothelial cell functions in response to vascular injury with the expectation that these functions can be regulated to affect these vascular responses in clinically relevant pathophysiological conditions was the goal for these studies.

Aim 1-We crossed $ApoE^{-/-}$ and $Bmper^{+/-}$ and measured the development of atherosclerosis in mice fed a high-fat diet. BMPER haploinsufficiency in $ApoE^{-/-}$ mice led to a more severe phenotype. Aim 2-$BMPER^{+/-}$ were used for LPS challenge. LPS-induced pulmonary inflammation and injury was reduced in $BMPER^{+/-}$ mice.

We conclude that BMPER is essential in the maintenance of normal vascular homeostasis during chronic inflammation and atherosclerosis. Furthermore, BMPER plays a pivotal role in pulmonary inflammatory response, to provides new therapeutic options against septic shock, and broadens our understanding of BMPER's role in vascular homeostasis.

TABLE OF CONTENTS

LIST OF FIGURES

LIST OF ABBREVIATIONS

ALI	Acute Lung Injury
ApoE	Apolipoprotein E
ARDS	Acute respiratory distress syndrome
BMP	Bone morphogenetic protein
BMPER	BMP-BINDING ENDOTHELIAL REGULATOR
CXCL10	CXC-ligand 10
EC	Endothelial cell
ECM	Extracellular matrix
eNOS	Endothelial nitric oxide synthase
ERK	Extracellular Signal-Regulated Kinase
GPCR	G-protein-coupled receptors
HUVEC	Human umbilical vein endothelial cell
ICAM1	Intracellular adhesion molecule 1
IEJ	Interendothelial junctions
IKK	IkB Kinase
IL-1	Interleukin-1
IL-10	Interleukin-10
IL-1ra	Interleukin-1 receptor agonist
IL-8	Interleukin-8
LDL	Low-density lipoprotein
LPB	LPS-binding protein

LPS	Lipopolysaccharide
LRP1	LDLR-related protein
LRR	Leucine-rich repeat
MAP	Mitogen-activated protein
MLEC	Mouse lung endothelial cells
NFAT	Nuclear factor of activated T cells
NFκB	Nuclear factor k light change enhance activated in B cells
NLS	Nuclear localization sequence
PAMP	Pathogen-associated molecular patterns
PKA	Phospho-kinase A
PRR	Pattern recognition receptors
RHD	Rel homology domain
TGF-β	Transforming growth factor-beta
TIL	Trypsin inhibitor-like
TJ	Tight junctions
TLR	Toll-like receptor
TNFα	Tumor necrosis factor a
VCAM1	Vascular cell adhesion molecule 1
VEGF	Vascular endothelial growth factor
VLDL	Very low-density lipoprotein
VWC	von Willebrand factor C
VWD	von Willebrand factor D

CHAPTER 1: GENERAL INTRODUCTION

1.1 THE ENDOTHELIUM IS A BIOLOGICALLY ACTIVE ORGAN

Blood vessels of the circulatory system, including arteries, veins and capillaries, form a network that transports nutrients and oxygen to all parts of the body. The endothelium, endothelial cells (EC) and their associated extracellular matrix, forms the inner lining of all blood vessels and lymphatic vessels in every organ system in the body. It was once believed to be an inert membrane whose only function was to provide a selectively permeable barrier to regulate the flow of water and nutrients to underlying tissues. However, a shift in this view began in the 1950s and 1960s. One important observation showed that lymphocytes were observed interacting with the endothelial layer surface, indicating the induction of a pro-adhesive, pro-coagulant EC phenotype by inflammatory mediators .[1–3] Since then, numerous studies have demonstrated that ECs have a central role in many physiologic processes, including the control of permeability, vascular tone, hemostasis and immune cell trafficking. The endothelium is also a central determinant in the pathophysiology of most if not at all diseases, either as a primary determinant of pathophysiology or as a contributory factor to collateral damage. These seminal studies brought about a paradigm shift that led to the current view of the endothelium as a dynamic paracrine and endocrine organ that plays a critical role in secretory, metabolic and immunologic functions. [1,4–7] However, there is a wide bench to bedside gap in endothelial cell medicine. One reason is likely due to the heterogeneous properties of the endothelium. Indeed, throughout the vascular tree endothelial cells show extensive heterogeneity in structure and function, in space and time as well as in health and disease. Despite recent studies our understanding of endothelial cell function

remains incomplete. Further studies of the signaling pathways associated with endothelial function are therefore critical in order to develop treatments for these vascular-associated conditions.

1.2 ENDOTHELIAL FUNCTION AND DYSFUNCTION

ECs play a critical role in vascular homeostasis by regulating many physiologic processes, such as vascular tone and permeability, proliferation, apoptosis, production and secretion of cytokines and vasoactive substances in response to stress and injury. ECs respond to different insults in an effective manner to maintain a healthy environment that is antithrombotic, anticoagulant and anti-inflammatory [1–3,8,9] Under physiologic conditions, ECs regulate vascular tone, blood pressure, and blood flow through the fine-tuned release of vasodilating factors such as nitric oxide and prostacyclins to counterbalance the vasoconstriction caused by endothelin and other vasocontrictors. To maintain an anticoagulant milieu, ECs release mediators of the tissue factor pathway and thrombomodulin inhibitors to inhibit activation of the procoagulant molecules thrombin, factor X and fibrin. [1,4,6,10,11] In addition to these many functions, ECs also regulate vascular homeostasis by responding to physical stimuli exerted on the surface of the endothelium. In this context, ECs function as hemodynamic sensors by responding to mechanical stimulation in the vessel wall that is produced by cyclic stretch and fluid shear stress to regulate signaling and gene expression. [3,9,10] However, when the endothelium fails to carry out any of these essential basal functions endothelial activation develops, and if it is not quickly resolved will result in endothelial dysfunction. Endothelial activation involves a phenotypic change of the resting ECs that promotes the pathological process such as inflammation, which contributes to the development of many diseases such as atherosclerosis, adult respiratory distress syndrome (ARDS), acute lung injury (ALI), and septic shock. [6,11,12]

Dynamic changes of permeability in the vessel wall are regulated by ECs and their associated extracellular matrix (ECM). The vascular endothelium provides a size selective,

semi-permeable barrier between circulating blood and underlying tissue and actively participates in blood-tissue exchange of fluid, ions, proteins and cells. Strict regulation of vascular permeability is required for many physiologic processes, including tissue-fluid homeostasis, angiogenesis, vessel tone and host defense.[13–15] Conversely, dysregulation of barrier function leads to endothelial hyperpermeability, a significant pathological event in many diseases, including atherosclerosis, ARDS and sepsis. ECs regulate the continuous movement of fluid, small solutes and macromolecules between the blood and underlying tissue using the transcellular and paracellular pathways. Water and small solutes less than 3 nm in diameter move through interendothelial junctions by way of the paracellular pathway, and the transcellular pathway transports larger molecules across the endothelium by vesicular-mediated transport. An important mechanism for transcellular permeability is caveolin-dependent transcytosis. Trancytosis is initiated following protein recognition by their membrane-receptors that are located in caveolae. Ligand-receptor binding activates caveolar fission; dynamin oligomers form around the caveolar neck and scission occurs when dynamin is hydrolyzed by GTP. The caveolae then move through the cytoplasm. The t-SNARE complex on the basolateral membrane mediates docking and fusion followed by exocytosis and release of the vesicular contents into the interstisial space.[13,15–17] Paracellular permeability is regulated by the dynamic opening closing of EC interendothelial junctions (IEJ). The IEJ complexes are formed by adherens junctions (AJ) and tight junctions (TJ). TJs contain claudin, occluding and junctional adhesion molecules. The transmembrane protein, VE-cadherin provides the molecular architecture of AJs. The extracellular portion of VE-cadherin tethers to VE-cadherin on adjacent cells, and members of the catenin family link the intracellular domain to the cytoskeleton. Paracellular permeability is then regulated through various mechanisms that cause phosphorylation, internalization, or degradation of the junctional proteins.[14–16,18]

Blood vessels are constantly subjected to various types of hemodynamic forces such as hydrostatic pressure, cyclic stretch, and fluid shear stress. Shear stress is the force per unit

area created by the tangential force of blood flow on the endothelial surface. The EC response to shear stress plays an important role in maintaining vascular homeostasis. Shear-induced mechanotransduction transforms mechanical forces to biochemical responses, activates signal transduction and endothelium-dependent gene and protein expression that determine endothelial cell phenotype. Steady laminar flow (10-50 dyn/cm2) promotes the release of factors from ECs that inhibit coagulation, leukocyte trafficking, and SMC proliferation while simultaneously promoting EC survival. In contrast, a dysfunctional endothelial phenotype that promotes atheroma formation is seen in areas of the arterial tree that promote disturbed flow e.g. curved regions, branch points and bifurcations.[4,11,19–24]

Endothelial dysfunction is a failure to perform any of the aforementioned physiological functions. The dysfunctional endothelium becomes pro-adhesive by expressing adhesion molecules on the surface, pro-thrombotic by activating circulating platelets and leukocytes, and pro-inflammatory by activating NFκB, NFAT and other signaling pathways. The dysfunctional endothelium is associated with a diverse assortment of disorders and diseases including Alzheimer's disease and neurological conditions associated with breakdown of the blood brain barrier, renal diseases, immune deficiencies, infections and of course many cardiovascular conditions. [5,11,20,22,25–27]

1.3 ROLE OF ENDOTHELIAL CELLS IN VASCULAR INFLAMMATION

1.3.1 INFLAMMATION

Inflammation, an integral part of the innate and adaptive immune system, is an important first-line of defense against infection, toxins and tissue injury. ECs are key regulators of the inflammatory process. They orchestrate complex interactions to generate the expression of cytokines, chemokines and adhesion molecules. These inflammatory factors in turn recruit plasma proteins, leukocytes and fluid to the injury site. ECs have a crucial role in the inflammatory process. Not only are ECs the first cells to come in contact

with the blood-born injurious agent, ECs receive and process signals from cytokines, chemokines and growth factors such as TNFα, IL-1, IL-8, MCP-1 and VEGF at the site of injury. ECs respond to these factors to influence the magnitude and timing of the resulting inflammatory response. ECs provide additional counter-regulatory mechanisms to protect the host from unrestrained inflammation and excessive tissue injury by responding to extrinsic anti-inflammatory signals of the anti-inflammatory cytokines, TGF-β, IL-10 and IL-1 receptor agonist (IL-1ra). A better understanding of how ECs respond to external anti-inflammatory signals and the pathways they use will help develop therapeutic options against inflammatory derived diseases.[11]

1.3.2 ACUTE INFLAMMATORY RESPONSE.

The innate immune system is the first line of host defense during injury or infection. As a result it plays a pivotal role in the early recognition and activation of the proinflammatory response to tissue injury or invading pathogens such as lung inflammation during septic shock. Two distinct types of EC activation characterize acute inflammation. Type I EC activation lasts for 10-20 minutes and uses G-protein-coupled receptors (GPCRs) to transduce several different intracellular signaling pathways that result in increased blood flow, vascular leakiness and neutrophil recruitment to the injury site. Type II endothelial activation provides a sustained response that can last hours or days and involves a change in gene expression in the injured ECs. [11,22]

To initiate the inflammatory response, innate immune cells recognize pathogen invasion or cell damage with either intracellular or surface-expressed pattern recognition receptors (PRRs). Pathogen-associated molecular patterns (PAMPs) are conserved structures on pathogens such as microbial nucleic acids, lipoproteins or carbohydrates that are recognized by PRRs. ECs are the first cells to interact with exogenous pathogens, and ECs are known to express toll-like receptors, a class of PRRs, on their surface. Recognition of PAMPs by TLRs on ECs activates expression of pro-inflammatory factors through the

initiation of signal transduction pathways that lead to the activation of mitogen-activated protein (MAP) kinase proteins and NF-κB. This then characterizes ECs both initiators and targets of the innate immune response. [28–32]

1.3.3 TOLL-LIKE RECEPTOR SIGNALING IN ENDOTHELIAL CELLS.

The Toll-like receptor (TLR) family is one of the most extensively studied PRR families that recognize PAMPs. TLRs are highly conserved across species and are characterized by an extracellular leucine-rich repeat (LRR) domain that mediates ligand binding, and a cytoplasmic IL-1 recepter homology (TIR) domain that serves as a docking site for TIR-containing cytoplasmic adaptor proteins. TLR1 through TLR10 are expressed in humans and mice, whereas TLR11 threough TLR13 are only expressed in mice. TLRs can be broadly divided into two major groups. TLR1, 2, 4, 5, 6 and 11 are cell membrane receptors, while TLR3, 7, 8, 9, 10 and 13 are confined to intracellular vesicles. The expression of TLRs is cell-type specific, and we know that ECs are a heterogeneous population of cells, expressing proteins that are vascular bed-specific. So for our purposes we will only discuss TLR4 signaling as it is widely expressed in ECs and has been most extensively studied. TLR4 is activated by lipopolysaccharide (LPS); LPS is a structural component of the outer membrane of Gram-negative bacteria and a classical pro-inflammatory stimulus in mouse sepsis shock models. [22,29,31,33]

LPS-binding protein (LPB) is the first host protein to interact with LPS in the extracellular space. LBP binds LPS and escorts it to the cell surface by binding CD14, a cell-surface receptor molecule. CD14 then transfers LPS to the TLR4/MD-2 receptor complex. Upon recognition of LPS, TLR4 recruits downstream signal transduction adaptor proteins. Activation of TLR4 leads to an early activation of NF-κB (MyD88-dependent) and a late-phase activation of NF-κB (MyD88-independent pathway).

Most TLR signaling is mediated through the MyD88 pathway, which is primarily responsible for regulating the expression of the inflammatory cytokines TNF□, IL-6 and IL-

12 via NF-κB activation. In response to LPS stimulation, MyD88 is recruited to the intercellular domain of TLR4. MyD88 then recruits IRAK4, which in turn binds to IRAK1. Auto-phosphorylation and activation of IRAK1 leads to IRAK1 binding TRAF6, an adapter protein, that forms a complex with UBC`13 and UEV1a which activates TAK1. TAK1 then activates NF-κB, MAPK and PI3 pathways to induce pro-inflammatory gene expression.

On the other hand, TIR-containing adaptor protein, TRIF, mediates MyD88 independent signaling that activates the transcription factor IRF3 and late phase NF-kB and MAPK activation. To initiate this pathway the adaptor molecule TRAM is recruited to the cytoplasmic domain of TLR4. TRAM then recruits TRIF and this leads more protein recruitment and a multiple protein complex with TRAF6, RIP1, NAP1 and TBK1 as members. TBK1 activates the transcription factor IRF3 and RIP1 mediates late phase NF-kB activation, leading to cytokine induction. [6,22,28,29,31,33,34]

1.3.4 NF-κB SIGNALING.

Induction of adhesion molecules and inflammatory cytokines are cardinal characteristics of endothelial activation. Nuclear factor kappa-light chain-enhancer of activated B cells (NF-κB) is a critical transcriptional regulator involved in the immune and inflammatory responses in many cell types including ECs. NF-κB describes various dimeric complexes of the Rel protein family. In mammals the Rel family has five members, NF-κB1 (p105/p50), NF-κB2 (p100/p52), Rel A (65), Rel B and c-Rel. These NF-κB proteins form many different homo- and hetero-dimers to regulate different transcriptional programs depending on the stimulus and cell type. Each of the five Rel family members has a Rel homology domain (RHD) in the N-terminus that is responsible for dimerization, nuclear translocation, DNA binding, and interaction with inhibitor of NF-κB (IκB).

In unstimulated cells the IkB family of inhibitor proteins sequester NF-κB in the cytoplasm. These IκB proteins bind the RHD and mask the C-terminal nuclear localization sequence (NLS). The IκB proteins are polyubiquitinated and marked for proteasome

degradation by IκB kinases that phosphorylate signal-dependent serines. The NLS is then exposed inducing NF-kB to translocate to the nucleus, bind DNA and regulate the expression of target genes.

NF-κB is activated by a wide range of agonists, such as microbial and viral pathogens, LPS, cytokines, low-density lipoprotein (LDL), very low-density lipoprotein (VLDL), angiotensin II (ANGII), glucose and disturbed flow. The pathogenesis of chronic inflammation and autoimmune disorders are often preceded by inappropriate NF-κB signaling.

1.3.5 ENDOTHELIAL CELL-DEPENDENT CHRONIC INFLAMMATORY RESPONSE.

The vascular endothelium is very versatile in nature and can alter its phenotype in response to the different phases of the inflammatory process. The adaptive immune response is triggered when innate immunity fails to resolve the injurious stimulus. The response will then progress from acute inflammation to chronic inflammation. During chronic inflammation, ECs modify their expression of adhesion molecules and chemokines; P-selectin, VCAM1 and ICAM1 are down-regulated, E-selectin is unchanged, and CXC-ligand 10 (CXCL10) is up-regulated. This modification promotes the interaction of ECs with type 1 T helper cells (Th1) that are not present during acute inflammation. [11]

1.4 BMP-BINDING ENDOTHELIAL CELL PRECURSOR-DERIVED REGULATOR

The BMPER gene encodes a 685 amino acid protein and has a molecular mass of 76.1 kDa. BMPER contains a 39 amino acid signal peptide followed by five closely spaced cysteine-rich von Willebrand factor C (VWC) domains in the N-terminal segment, and the C-terminal portion has a von Willebrand factor D (VWD) domain and a trypsin inhibitor-like (TIL) domain. BMPER was originally identified in a screen for differentially expressed protein in developing embryoid bodies and is highly conserved across species.35 The

BMPER mouse homolog share 92 percent, zebrafish share 65 percent and drosophila share 38 percent sequence homology with human BMPER.

BMPER, through its regulation of the BMP signaling events, is critically involved in numerous aspects of EC biology that affect development in the embryo, revascularization in adult tissues, and vascular inflammation. BMPs mediate a diverse range of functions during vertebrate development, including left-right embryonic asymmety, neurogenesis, mesoderm patterning, organogenesis and cellular differentiation. BMPER binds BMPs through the first VWC domain in the N-terminal region with a 2:1 stochiometry and has both pro-and anti-BMP activities. [36–38]

BMPER regulates BMP activity in a tissue and stage-dependent manner. In Drosophila the BMPER homolog, Crossveinless 2 (Cv-2), is required for signaling by the BMP orthologs, Dpp and Gbb. Loss of Cv2 in Drosophila results in the failure to form cross veins in the wing. Injection of BMPER mRNA into the Xenopus embryo results in formation of a secondary axis due to inhibition of BMP signaling. In zebrafish zbmper is expressed at sites of high BMP activity, while morpholino knockdown of zbmper resulted in a dorsalized phenotype, dysmorphic caudal vein plexus, aberrant intersegmental vessel formation and reduced numbers of circulating blood cells. BMPER-/- mutant mice are perinatal lethal and embryologic studies reveal BMPER-/- mice have cardiac valve, lung, skeletal, eye and kidney developmental defects. [35,39,40]

BMPER has been identified as a novel protective regulator of vascular inflammation and vascular diseases. Previous studies have identified a regulatory role for BMPER in the inflammatory response through its regulation of BMP signaling. BMP4 is well established as an inflammatory cytokine, and promotes the inflammatory response in the endothelium. BMP4 upregulates the inflammatory molecules ICAM1 and VCAM1 on the surface of the endothelium, and BMP4 is induced in atheroprone regions of disturbed blow such as branches, bends and bifurcations of the vasculature in vivo. BMPER and other extracellular BMP regulators are upregulated in these regions as well. Reports also show that BMPER is

induced by inflammatory-regulatory stimuli such as oscillatory shear stress and mevastatin, and inhibits TNFα-induced endothelial inflammation. [35,41–45]

BMPER-dependent signaling responses in the endothelium have been characterized by us, and others, firmly establishing a role for BMPER in regulating vascular responses to stress in physiologic conditions.[40,42,43,46–53] Our laboratory has characterized BMPER's involvement in BMP signaling events associated with vascular development and revascularization in adult tissue. Our characterization of BMPER-dependent endothelial signaling responses have firmly established a role for BMPER in regulating vascular responses to stress in physiologic systems.[40,42,43,47,54] Currently, mechanistic details of BMPERs regulation of the vascular response to injury, and the signaling pathways involved is very limited. Our overall goal is to determine how BMPER-mediated signaling events contribute to the regulation of endothelial cell functions in response to vascular injury with the expectation that these functions can be regulated to affect these vascular responses in clinically relevant pathophysiologic conditions.

CHAPTER 2: BMPER INHIBITS ENDOTHELIAL EXPRESSION OF INFLAMMATORY ADHESION MOLECULES

2.1 INTRODUCTION

Atherosclerosis is a disease that results from plaque formation within arteries, resulting in arterial hardening and narrowing. It is mediated by a chronic inflammatory process characterized by the accumulation of lipids and inflammatory cells (plaque) along the inner walls of arteries.[1] Although plaque formation is a complex process, endothelial inflammation has been identified as one of the critical initiating factors.[1] Endothelial inflammation can be induced by decreases or disruptions in blood flow, making some regions of the vasculature more prone to plaque formation.[2,3] For example, arterial regions that are exposed to uniform, unidirectional blood flow with high shear stress are protected from endothelial inflammation and have a lower incidence of atherosclerotic plaque formation.[3,4] In comparison, atherosclerotic lesions develop predominantly at branches, bends, and bifurcations in arteries,[5–7] where endothelial cells are exposed to low or disturbed fluid shear stress, resulting in low mean and oscillatory shear stress on the endothelial cells. In these lesion-prone regions, disturbed or oscillatory shear stress increases expression of bone morphogenetic proteins (BMPs) and their antagonists in the vascular endothelium.[8,9] In turn, BMPs activate an inflammatory response characterized by the expression of adhesion molecules, like intracellular adhesion molecule 1 (ICAM1) and vascular cell adhesion molecule 1 (VCAM1) on the endothelial surface.[9] Despite this, animal studies examining the direct role of bone morphogenetic protein (BMP) on vascular inflammation have been inconclusive, with some studies reporting a decrease in inflammatory responses and

atherosclerotic lesion formation when BMP activity is increased,[10] whereas others conclude that BMP plays a proinflammatory role.[10,11] Although each of these studies support a central role for BMP-mediated endothelial inflammation in atherosclerosis, some uncertainty remains about the precise contribution of BMP signaling to endothelial inflammation and atherosclerosis. BMPs belong to the transforming growth factor-β superfamily and play important roles in cellular processes, such as bone formation, proliferation, differentiation, motility, vasculogenesis, and angiogenesis (reviewed by Moreno-Miralles[12]). More specifically, BMP4, together with BMP2 and BMP6, demonstrate important roles in endothelial differentiation, migration, and angiogenesis.[13–16] Previously we identified BMPER, a novel extracellular modulator of BMP signaling, which is required for hematopoietic and vascular development and hypoxia–induced retinal neovascularization.[13,14,17] We have also demonstrated that BMPER regulates BMP4 activity in a dose-dependent manner.[13] Recent reports show that BMPER is induced by inflammatory-regulatory stimuli, such as oscillatory shear stress and mevastatin, and inhibits tumor necrosis factor-α–induced endothelial inflammation,[18,19] suggesting that BMPER acts in an anti-inflammatory capacity in endothelial cells by inhibiting BMP activity. This led us to question whether BMPER may also inhibit the endothelial inflammation and subsequent pathology associated with atherosclerosis. In this study, we used the apolipoprotein E–deficient ($ApoE^{-/-}$) mouse atherosclerotic model to study the effects of BMPER haploinsufficiency on the development of atherosclerosis. We used $BMPER^{+/-}$ mice instead of $BMPER^{-/-}$ mice because $BMPER^{-/-}$ mice die at birth.[13] $BMPER^{+/-}$;$ApoE^{-/-}$ mice fed a high-fat (HF) diet displayed an exacerbated inflammatory vascular response compared with $ApoE^{-/-}$ mice with the wild-type BMPER gene ($BMPER^{+/+}$/$ApoE^{-/-}$). Mechanistically, we demonstrate that BMPER exerts protective effects by inhibiting BMP activity. These data demonstrate for the first time that BMPER is a novel player in the development of atherosclerosis and in fluid shear stress–modulated inflammatory responses in endothelial

cells. Taken together, it suggests that BMPER is a novel protective regulator of vascular inflammation and vascular diseases, such as atherosclerosis.

2.2 RESULTS

2.2.1 BMPER Expression Protects Against Atherosclerotic Lesion Formation and Calcification

Accumulated evidence suggests that BMPER protects endothelial cells from inflammation by inhibiting BMP activity.[18,19] Therefore, we used the ApoE$^{-/-}$ mouse model, in which a HF diet leads to accelerated atherosclerotic lesion formation and arterial calcification, to analyze the in vivo effect of reduced BMPER expression on vascular inflammation. We crossed wild-type or ApoE$^{-/-}$ mice with mice that had either 1 or 2 functional BMPER alleles, resulting in 4 genotypes of experimental mice: BMPER$^{+/+}$/ApoE$^{+/+}$, BMPER$^{+/-}$/ApoE$^{+/+}$, BMPER$^{+/+}$/ApoE$^{-/-}$, BMPER$^{+/-}$/ApoE$^{-/-}$. These mice were then fed either a standard chow or HF diet for 20 weeks, and the formation of atherosclerotic plaques in the aorta and aortic sinus regions was evaluated by Oil Red O staining. ApoE$^{-/-}$ mice that were haploinsufficient for BMPER expression (BMPER$^{+/-}$/ApoE$^{-/-}$) responded to the HF diet with enhanced plaque formation compared with BMPER$^{+/+}$/ApoE$^{-/-}$ mice (28.35 ± 2.23% versus 17.96 ± 3.00%, P=0.016), as measured by *en face* staining of aortic lesions (including both thoracic and abdominal aorta, Figure 2.1 A and 2.1B). In addition, cross-sectional analysis of aortic sinus lesions revealed that the plaques formed in the BMPER$^{+/-}$/ApoE$^{-/-}$ mice were larger compared with lesions in BMPER$^{+/+}$/ApoE$^{-/-}$ mice (0.38 ± 0.02% versus 0.29 ± 0.03%, P=0.018), demonstrating a protective effect of BMPER expression on the degree of plaque growth (Figure 2.1C and 2.1D). When lesion calcification was compared between genotypes, BMPER$^{+/-}$/ApoE$^{-/-}$ mice again showed an exacerbated response, with a 120% increase over baseline levels of calcification as determined by von Kossa staining, compared with a 68% increase in the BMPER$^{+/+}$/ApoE$^{-/-}$ mice. This equated to an overall increase in total calcification of 1.12 ±

0.25% in BMPER$^{+/-}$/ApoE$^{-/-}$ mice versus 0.37 ± 0.22% in BMPER$^{+/+}$/ApoE$^{-/-}$ mice (Figure 2.1E and 2.1F). BMPER$^{+/-}$/ApoE$^{-/-}$ mice fed the HF diet showed no differences in body weight or serum cholesterol levels compared with BMPER$^{+/+}$/ApoE$^{-/-}$ mice (Figure 2.6 A and 2.6 B), indicating that diet induced increases in weight and lipid levels are not responsible for the more robust atherosclerotic phenotype in the BMPER$^{+/-}$/ApoE$^{-/-}$ mice. Together, these results indicate that BMPER plays a protective role in plaque formation and arterial calcification in an in vivo model of atherosclerosis.

2.2.2 BMPER Expression Inhibits Aortic Inflammation

Several reports have demonstrated a central role for the BMP signaling pathway in promoting endothelial inflammatory responses.[8,9,18–20] Therefore, we sought to determine whether the protective influence of BMPER on the development of atherosclerotic lesions is attributable to changes in vascular inflammation. To test this, we measured the degree of macrophage infiltration (a common phenotype observed with the onset of atherosclerotic plaques) and expression of inflammatory markers in atherosclerotic plaques in BMPER$^{+/+}$/ApoE$^{-/-}$ and BMPER$^{+/-}$/ApoE$^{-/-}$ mice. Quantitative analysis revealed a more robust degree of macrophage infiltration (determined by CD68 expression) in aortas of BMPER$^{+/-}$/ApoE$^{-/-}$ mice compared with BMPER$^{+/+}$/ApoE$^{-/-}$ mice (0.143 ± 0.016% CD68-positive area per aortic cross-sectional area versus 0.057 ± 0.013%, respectively) after 20 weeks of the HF diet (Figure 2.2 A and 2.2 B). BMPER$^{+/-}$/ApoE$^{-/-}$ mice also exhibited a dramatic increase in the expression of 2 inflammatory markers, ICAM1 and VCAM1, in the intima associated with aortic lesions, compared with BMPER$^{+/+}$/ApoE$^{-/-}$ mice after 20 weeks of the HF diet (Figure 2.2 C, D, E and F), supporting the notion that BMPER functions as an anti-inflammatory mediator. Similar increases in ICAM1 and VCAM1 expression were also observed in serum from BMPER$^{+/-}$/ApoE$^{-/-}$ mice compared with BMPER$^{+/+}$/ApoE$^{-/-}$ mice after 4 weeks of the HF diet (Figure 2.7). We also performed immunostaining with anti-BMPER and ANTI-BMP4 antibodies to determine whether there is a change in the level of

expression of these proteins in response to vascular inflammation induced by HF diet. We observed a robust increase in BMPER (Figure 2.8 A) and BMP4 (Figure 2.8 B) levels in mice fed a HF diet compared with those fed a control diet. This increase in BMPER and BMP4 correlated with the increased expression of ICAM1/VCAM1 and CD68 signals (Figure 2.2), further supporting the notion that the modulation of BMP signaling by BMPER plays an important role in the inflammatory responses induced by HF diet. Collectively, these data demonstrate that BMPER haploinsufficiency leads to phenotypic changes correlative with an increased chronic, vascular inflammatory response and likely contributes to the aggravated atherosclerotic lesion formation observed in the $BMPER^{+/-}/ApoE^{-/-}$ mice.

2.2.3 BMPER Inhibits Shear Stress–Dependent Induction of Inflammatory Adhesion Molecules in the Endothelium

Aortic lesions develop predominantly in regions that are exposed to low or disturbed fluid shear stress, such as the LC of the aorta. Even under normal hemodynamic conditions, previous studies demonstrate higher endothelial inflammation in the LC compared with other regions of the aorta, such as the GC,[3,4] possibly because of the increased expression of BMPs in the vascular endothelium of these regions.[8] This difference in lesion formation in the GC and LC was also observed in the BMPER atherosclerosis model. Specifically, we observed that there was a very significant increase in lesion area in the LC compared with GC of both $BMPER^{+/+}/ApoE^{-/-}$ and $BMPER^{+/-}/ApoE^{-/-}$ mice (Figure 2.9). Immunostaining of the cross sections of the LC and GC with an antibody specific for BMPER demonstrated a dramatic increase of BMPER protein levels in the intima and media of the LC compared with the GC in both $BMPER^{+/+}$ and $BMPER^{+/-}$ mice (Figure 2.10). To quantitatively determine the difference of BMPER protein level in the GC and LC, we also performed Western blotting with vessel lysates obtained from the GC and LC. We observed significantly more BMPER protein located in the LC than GC in both $BMPER^{+/+}$ and $BMPER^{+/-}$ mice (Figure 2.10B), suggesting that BMPER protein level is modulated by different fluid shear stress. High shear stress in the LC decreases BMPER leading to a decrease in lesion size. Encouraged by these

observations, we used this inherent difference in BMPER expression between the LC and GC to analyze the effect of reduced BMPER expression on downstream mediators and effectors of BMP activation in these regions of mouse aortas. To simplify our experimental setup, we only examined mice on the ApoE$^{+/+}$ background. Endothelial cells located in the LC region of aortas of BMPER$^{+/+}$ mice displayed abundant Smad1, 5, and 8 activation (as detected by phosphorylated Smad1, 5, and 8 signals) compared with endothelial cells in the GC region (Figure 2.3A), consistent with previous reports. In contrast, BMPER$^{+/-}$ mice exhibited an enhanced increase in Smad activation in the LC region in comparison with BMPER$^{+/+}$ mice; but in addition, BMPER$^{+/-}$ mice had clearly detectable Smad activation in the GC region of the aortas, consistent with our *in vivo* data described above indicating that BMPER functions as an anti-inflammatory mediator (Figure 2.3B). Expression patterns of both ICAM1 and VCAM1 paralleled that of Smad activation (Figure 2.3C–2.3F), demonstrating that BMPER inhibits the endothelial response to oscillatory shear stress–mediated induction of endothelial inflammatory adhesion molecules, and in the context of atherosclerosis, may directly inhibit the endothelial inflammatory response.

2.2.4 BMPER Inhibits BMP4-Induced Inflammatory Gene Expression in Endothelial Cells and Prevents Fluid Shear Stress–Induced Inflammatory Responses

Our *in vivo* results clearly support a role for BMPER in suppressing shear stress–mediated inflammation. To determine the effects of BMPER on inflammation in the endothelial cell compartment, we established a cell-based model to determine whether BMPER's ability to attenuate inflammation is BMP4 dependent and is in response to fluid shear stress. Treatment of primary HUVECs with BMP4 increased ICAM1 and VCAM1 expression at both the RNA and protein levels in a time-dependent manner, with peak expression occurring at 8 hours post-treatment (Figure 2.4A and 2.4B and data not shown), consistent with the previous reports. This robust BMP4-mediated increase in ICAM1 and VCAM1 expression was blocked in the presence of exogenous BMPER (Figure 2.4C),

demonstrating that BMPER directly antagonizes BMP4-mediated inflammatory signaling. Next, we examined the ability of endogenous BMP4 and BMPER to affect the expression of inflammatory markers. Given the robust inflammation seen in the normally quiescent GC region of the aorta in $BMPER^{+/-}/ApoE^{-/-}$ mice, we hypothesized that reducing endogenous BMP4 or BMPER expression in endothelial cells would affect the inflammatory signature of the cells even in the absence of exogenous mediators. As expected, BMP4-targeted siRNA reduced expression of ICAM1 and VCAM1 in transfected cells, whereas siRNA-mediated reduction of endogenous BMPER expression resulted in a significant increase in these same inflammatory markers (Figure 2.4D and 2.4E). Collectively, our data demonstrate that the anti-inflammatory function of BMPER in endothelial cells is mediated, at least in part, through antagonizing BMP activity.

Given the effect of BMPER gene dosage on endothelial inflammation *in vivo* (Figure 2.3) and the *in vitro* effects of a reduction of BMPER expression on endothelial inflammation in the absence of any stimuli (Figure 2.4), we hypothesized that the inflammatory response to shear stress in the aorta may be mediated by changes in the levels of BMPER expression. To test this hypothesis directly, we subjected HUVECs to conditions that mimic the shear stress conditions in the LC and GC aortic regions using either oscillatory stress (±5 dyne cm−2) or laminar shear stress (20 dyne cm−2) for 8 hours, respectively. Consistent with our *in vivo* data, endothelial cells subjected to oscillatory shear had a larger inflammatory response (a 2.33-fold and 4.56-fold increase in ICAM1 and VCAM1 expression, respectively) compared with cells subjected to laminar shear, respectively (Figure 2.5A). Interestingly, we also observed increases in BMP4 and BMPER expression in oscillatory shear conditions compared with laminar shear conditions (Figure 2.5A). Moreover, the protein ratio of BMP4 to BMPER increased more dramatically in oscillatory shear conditions compared with laminar shear conditions (Figure 2.5B). To determine whether the inflammatory response observed in our shear stress model is mediated by changes in BMPER protein level, we used siRNA-mediated gene silencing of BMPER and compared the extent of inflammatory marker

expression with control siRNA-treated cells. In control siRNA-treated cells, we detected higher ICAM1 and VCAM1 expression after oscillatory shear was compared with laminar shear (Figure2. 5C–2.5E), with similar patterns of BMP4 and BMPER expression as what was seen in untreated cells exposed to both modes of shear stress (Figure 2.5A). In BMPER siRNA-treated cells, we observed an increased inflammatory response in oscillatory shear conditions compared with control siRNA–treated cells (Figure 2.5C–2.5E), consistent with the increased inflammation we observed in the LC regions of $BMPER^{+/-}$ aortas (Figure 2.3). Additionally, even in the low inflammatory environment (laminar shear stress), reducing BMPER expression resulted in 34% and 68% higher expression of ICAM1 and VCAM1, respectively, compared with control siRNA– treated cells (Figure 2.5C–2.5E), paralleling our observations seen in the GC regions of $BMPER^{+/-}$ aortas (Figure 2.3). Given that laminar shear stress promotes endothelial survival and integrity by activating endothelial nitric oxide synthase (eNOS) signaling[4] and that BMPER regulates eNOS protein expression and activity under static conditions,[19] we tested whether eNOS is regulated by BMPER under laminar or oscillatory shear conditions. Very excitingly, we observed that control siRNA–treated endothelial cells subjected to laminar shear stress for 8 hours displayed a robust increase in eNOS phosphorylation compared with cells subjected to oscillatory shear stress (Figure 2.5F and 2.5G). However, in BMPER siRNA–treated cells, we observed a significant decrease in eNOS phosphorylation (Figure 2.5F and 2.5G) after laminar shear compared with the control-treated cells. This suggests that the protective effect of BMPER under laminar shear conditions might be mediated by increased eNOS activity. The detailed mechanism behind this eNOS regulation by BMPER under laminar shear conditions remains to be determined. Taken together, these data demonstrate a protective role for BMPER in laminar shear stress environments to reduce endothelial inflammation.

2.3 DISCUSSION

In this study, we have identified a previously unrecognized, protective role for BMPER in the setting of atherosclerosis. $ApoE^{-/-}$ mice, which develop an atherosclerotic phenotype when fed a HF diet, displayed significantly worsened symptoms when they carried only 1 phenocopy of the BMPER gene ($BMPER^{+/-}$;$ApoE^{-/-}$ mice). Not only did the decrease in BMPER levels in these mice cause a dramatic increase in lesion size, it also resulted in increased arterial calcification and a heightened induction of endothelial inflammatory adhesion molecules in the aorta in regions subjected to oscillatory and laminar shear stress. Similar results were found in cultured cell studies, solidifying the notion that BMPER is a critical regulator of vascular inflammation and broadening our understanding of the role that BMPER plays in the myriad events that result from the BMP signaling pathway.

Previously, our studies revealed the essential roles of BMP and BMPER signaling in endothelial cell differentiation, migration, and angiogenesis.[13,14,16,17,21,22] With the results from the present study, we can now add vascular inflammation to the growing list of BMP signaling events that are regulated by BMPER. $BMPER^{+/-}$ mice demonstrated increased Smad activation and expression of the inflammatory markers ICAM1 and VCAM1 in the endothelium layer of the LC of the aorta, a region known to be predisposed to atherogenic activity attributable to the BMP-mediated vascular inflammation brought about by oscillatory shear stress effects on endothelial cells (Figure 2.3). In addition, decreased levels of BMPER in $BMPER^{+/-}/ApoE^{-/-}$ mice led to an increase in the number of macrophages that were recruited and that migrated to the inflamed, atherogenic regions of the aortas (Figure 2.2A and 2.2B), supporting the notion that BMPER acts as a protective regulator of vascular inflammation. It is worth noting, however, that BMPER may also play a role in maintaining general vascular health in addition to its role in inflammatory responses. Our analysis of aortas taken from $ApoE^{+/+}$ mice that were haploinsufficient for BMPER ($BMPER^{+/-}/ApoE^{+/+}$ mice) revealed a significant increase in the area of atherosclerotic lesions in mouse fed a

regular diet (Figure 2.1A and 2.1B). This suggests that BMPER may be important in maintaining vascular health even under basal conditions, a theory that will require further experiments to determine.

As compelling as these *in vivo* results are, however, it is important to remember that the decrease in BMPER expression in the BMPER$^{+/-}$ mouse is not limited to endothelial cells. Because atherosclerosis is a pathological condition that results from the dysfunction of multiple cell types and involves different cellular events, it is not possible, from these *in vivo* studies, to localize the protective effect of BMPER to endothelial cells alone. Indeed, published reports demonstrate that BMPs enhance smooth muscle cell migration and induce proinflammatory factors, such as inducible nitric oxide synthase and tumor necrosis factor in macrophages.[23,24] The inhibition of BMP activity by specific inhibitors and antagonist decreases vascular calcification, suggesting important roles of BMP in vascular calcification, as well as early vascular injury. Therefore, it is entirely possible that BMPER, a secreted extracellular BMP modulator, may also be able to influence BMP activity not only in endothelial cells but in additional cell types such as smooth muscle cells and macrophages. Therefore, the contribution of BMPER to protection against atherogenic processes and vascular inflammation will need further investigation.

As mentioned above, a number of published reports have detailed the role of BMPER/BMP signaling in various aspects of endothelial cell function.[13,14,16,17,21,22] However, the ability of BMPER to inhibit endothelial inflammatory responses has not been investigated directly. To examine this aspect of endothelial BMP signaling, we cultured HUVECs and subjected them to fluid shear stress to induce an inflammatory response similar to what occurs within atherogenic areas of the aorta. We found that BMPER inhibits the inflammatory response usually elicited from endothelial cells in response to oscillatory shear stress (Figures 2.3 and 2.5). This result is consistent with other reports demonstrating that the expression of BMPER and other BMP antagonists is increased by oscillatory shear stress compared with laminar shear stress.[8] Surprisingly, we found that BMPER also exerts an anti-

inflammatory effect on endothelial cells exposed to laminar shear stress. Laminar shear stress promotes endothelial survival and integrity by activating mitogen activated protein kinases, such as extracellular-signal regulated kinase/big mitogen-activated protein kinase 1 and endothelial NOS signaling.[4] Our data demonstrated that BMPER is also involved in protecting endothelial cells exposed to laminar shear stress, partly, because of increases in the activity of eNOS and decreases ICAM1 and VCAM1 expression (Figure 2.5C and 2.5F) that have recently been attributed to BMPER activity in endothelial cells.[19] The exact molecular mechanism through which BMPER modulates eNOS activity and other signaling pathways of laminar shear stress need further investigation. BMPER has been identified as a critical regulator of BMP signaling activity, important in both vascular development and in hypoxia-induced retinal neovascularization.[13,14] Previously, we reported a gradient effect of BMPER's ability to influence BMP signaling, whereby superstoichiometric concentrations of BMPER compared with BMP inhibit BMP signaling and substoichiometric concentrations of BMPER compared with BMP activate BMP signaling.[13] In this study, we observed 61% and 15% higher BMP4 and BMPER expression in oscillatory shear stress conditions, resulting in a significantly lower BMPER to BMP4 ratio compared with laminar shear stress conditions, an expression pattern consistent with an anti-inflammatory role for BMPER (Figure 2.5A and 2.5B). This observation further suggests that the fine-tuning of BMP activity by BMPER is essential for modulating BMP-mediated cellular functions. Collectively, the data presented in this report demonstrate that the regulation of BMP activity by BMPER is essential for the maintenance of normal vascular homeostasis (Figure 2.11) and its disruption increases the risk of inflammatory vascular diseases, such as atherosclerosis.

2.4 MATERIALS AND METHODS

2.4.1 ANIMALS AND DIETS

ApoE$^{-/-}$ mice on C57BL/6J background were kindly provided by Dr. Maeda (UNC, Chapel Hill, NC). BMPER$^{+/-}$ mice, previously generated in our laboratory on a C57BL/6J

genetic background1, were crossed with ApoE$^{-/-}$ mice to generate BMPER$^{+/-}$/ApoE$^{-/-}$ mice. We used the BMPER$^{+/-}$ mice instead of BMPER$^{-/-}$ mice because BMPER$^{-/-}$ mice die at birth. All adult mice were fed with the standard chow or a high-fat/highcholesterol diet (Western diet) (Harlan Laboratories, Indianapolis, IN) for 20 weeks. Body weight of mice was monitored before and after they were fed with different diets. Blood serum was obtained every four weeks. All mouse experimental procedures were performed according to the National Institutes of Health *Guide for the Care and Use of Laboratory Animals* and approved by the Institutional Committee for the Use of Animals in Research.

2.4.2 LIPID ANALYSIS

Mice were fasted for 18 hours before blood sampling. Less than 200 μL of blood was collected through submandibular bleeding using a lancet. The total cholesterol level was measured enzymatically with a commercially available kit (Infinity kits, Thermo Scientific, Waltham, MA).

2.4.3 LESION QUANTIFICATION

The mice were euthanized and perfusion fixed with 10% buffered formalin via the left ventricle for 5 minutes. The lesions located in the aorta and aortic sinuses were analyzed using Oil Red O staining. To measure lesions in the aorta, the whole aorta, including the ascending arch, thoracic, and abdominal segments, was dissected, gently cleaned of adventitial tissue, and stained with Oil Red O (Sigma, St. Louis, MO). The surface lesion area was quantified with ImageJ software (Version 1.42q, NIH, Bethesda, MD) and is presented as a percentage of the total surface area of the whole aorta. To measure the lesions in the aortic sinuses, the heart and proximal aorta were excised, and the apex and lower half of the ventricles were removed. The remaining sample was embedded in optimal cutting temperature (OCT) compound (Tissue-Tek, Fisher Scientific, Pittsburgh, PA) and frozen on dry ice. Starting from the appearance of the aortic valve, serial frozen sections at 5 μm thickness were collected until the aortic valves were completely sectioned after the

previously described protocol. Twenty sections were stained with eosin and Oil Red O. The slides were imaged by light microscopy, and the atherosclerotic lesion area located in aortic sinus area was quantified with ImageJ and averaged over a 280 μm region.

2.4.4 Calcification Quantification

Deposited calcium in the aorta was detected by staining with von Kossa. The 5 μm cryosections of aortic sinus were prepared as described above and subjected to the von Kossa staining procedure. The calcification area from each section was quantified as a percentage of the total vessel cross-sectional area using ImageJ software.

2.4.5 ELISA Measurements

Blood samples were drawn from mice after consuming the HF diet or standard chow for 4 weeks. Soluble VCAM and soluble ICAM were measured in plasma in triplicate using an ELISA method (R&D Systems Minneapolis, MN).

2.4.6 Reagents

Recombinant human BMP4 and BMPER protein and antibodies recognizing BMPER and BMP4 were obtained from R&D Systems. VCAM1 antibodies were obtained from Santa Cruz Biotechnology (Santa Cruz, CA) for Western blotting and Chemicon for immunofluorescence (Millipore, Billerica, MA). The ICAM1 antibody was purchased from Cell Signaling Technology (Danvers, MA) and was used for Western blotting experiments. An additional ICAM1 antibody (purchased from Chemicon) was used for immunofluorescence experiments. The phosphorylated Smad1, 5, and 8 antibodies were purchased from Cell Signaling Technology and used for both Western blotting and immunofluorescence experiments.

2.4.7 Cell Culture and siRNA Transfection

Human umbilical vein endothelial cells (HUVECs) were purchased from Lonza and cultured in endothelial basal medium (EBM; Lonza, Allendale, NJ) supplemented with

hydrocortisone, bovine brain extract, epidermal growth factor, and 2% fetal calf serum. The cells from passages 4–8 were used for experiments. The stealth small interfering RNA (siRNA) duplexes were obtained from Invitrogen (Grand Island, NY). The siRNAs against mouse BMPER are a mixture of the duplexes of 5′GAAUUUCAGCCAGAAGGAAGCAAAU-3′ and 5′-GGAGAGAUGUGGUCCUCUAUCAAUU-3′. The siRNA against mouse BMP4 is a duplex of 5′-GCAUGUCAGGAUUAGCCGAUCGUUA-3′. The control siRNA is the Stealth RNAi negative control duplex (Cat. No. 12935-300) and was purchased from Invitrogen. The siRNAs were transfected into HUVECs according to the manufacturer's recommended protocol for Nucleofection (Lonza, Walkersville, MD; the HUVEC protocol). Briefly, for each sample, 2×10^5 HUVECs were transfected with 300 pmol siRNA. The experiments with BMP4 or BMPER siRNA-transfected HUVECs were performed 1 day or 4 days later, respectively. The siRNAs resulted in more than 70 percent knockdown of the protein levels of BMP4 and BMPER.

2.4.8 SHEAR STRESS ASSAYS

HUVECs were post-confluent for 48 hours before the performance of fluid shear stress experiment to decrease the background signal. Laminar shear stress assay was described previously. Briefly, confluent cells in a 10-cm dish were exposed to shear stress using the cone- and plate-flow chamber system for 8 hours at 20 dyne/cm^2 for laminar shear stress or ± 5 dyne/cm^2 for oscillatory shear stress experiments.

2.4.9 IMMUNOBLOTTING

Cells were harvested in lysis buffer (1% Triton X-100, 50 mmol/L Tris (pH 7.4), 150 mmol/L NaCl, 1 mmol/L Na3VO4, and 0.1% protease inhibitor mixture; Sigma) and clarified by centrifugation at 16,000 g. Proteins were separated by SDS-PAGE and transferred to nitrocellulose membranes.

2.4.10 IMMUNOFLUORESCENCE

The aortic arch segments were dissected out and gently cleaned of the adventitia. The aortic fragments located at the greater curvature (GC) and lesser curvature (LC) were separated and fixed in 3.7% formaldehyde for 10 minutes at room temperature. The aortic fragments were sequentially treated with 70% ethanol for 30 minutes and 5% hydrogen peroxide in methanol. Then, the segments were washed with water for 5 minutes. For the phosphorylated Smad1, 5, and 8 antibody, the samples were soaked in boiling citric acid buffer (10 mmol/L; pH, 6.0) for 9 minutes to expose the antigens. Next, the aortic fragments or 5 μm cryosections of the aortic root were blocked with 5% heat-inactivated goat serum for 1 hour and then incubated overnight with primary antibodies against ICAM1, VCAM1, CD31, or CD68 diluted in the blocking solution. After 3 washes in tris buffered saline, cells were incubated in the dark with a second antibody conjugated with Alexa Fluor 488 or 568 (Molecular Probes, Eugene, OR) in blocking solution for 90 minutes at 37°C. After 3 washes in tris buffered saline, the fragments were counterstained with DAPI for phosphorylated Smad1, 5, and 8 staining. The *en face* images of the endothelial layer and the cross-sectional images of the aortic root were visualized by confocal laser scanning microscopy.

2.4.11 IMMUNOHISTOCHEMISTRY

The aortic arch segments were dissected out and gently cleaned of the adventitia. The aortic fragments located at the greater curvature (GC) and lesser curvature (LC) were separated and fixed in 3.7% formaldehyde for 10 minutes at room temperature. After incubating tissue in a sucrose gradient, aortic samples were embedded in OCT compound and submitted for frozen sectioning. For the anti-BMPER and BMP4 antibody, the samples were soaked in boiling citric acid buffer (10 mmol/L, pH 6.0) for 10 minutes to expose the antigens. Next, the 5 μm cryosections of the aortic root or aortic arch were blocked with 5% heat inactivated rabbit serum for 1 hour and then incubated overnight with primary antibodies against BMPER or BMP4 antibodies diluted in the blocking solution. After three

washes in TBS, samples were incubated in a second antibody. For BMPER staining, we utilized amplification processes including the serial incubation with ABC (Vector Labs, Burlingame, CA, USA) and tyramide signal amplification reagent (Waltham, MA, USA) in blocking solution for 30 minutes for each at 37 °C. After 3 washes in TBS, the sections stained with BMPER and BMP4 antibodies were developed with DAB. The images were recorded using the bright field microscopy with 10x and 20x objective lens.

2.4.12 Statistical Analysis

Data are shown as the mean ± SE for 3 to 4 separate experiments. Differences were analyzed with 2-way ANOVA and post hoc analyses such as Student t-test when needed. Values of $P \leq 0.05$ were considered statistically significant.

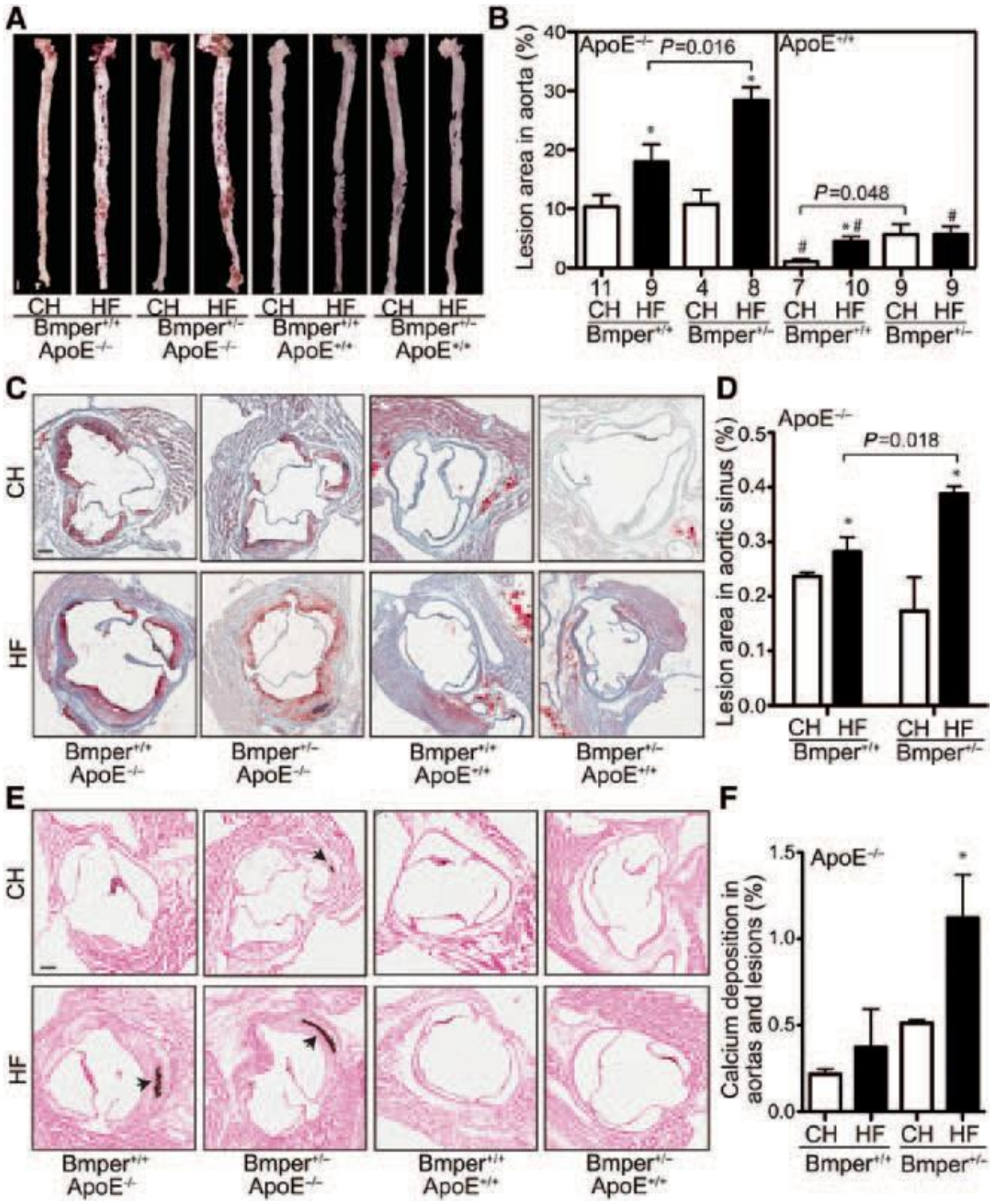

Figure 2-1. BMPER haploinsufficiency leads to aggravated atherosclerotic plaque formation.

Mice were fed a high-fat diet (HF) or standard chow (CH) for 20 weeks. The aorta and heart were dissected out and stained with Oil Red O. (A) Representative images of the Oil Red O staining of aortas. Scale bar, 1.5 mm. (B) The lesions on the surface of each aorta were quantified as a

percentage of the total area of the aorta. *P<0.05, compared with mice with the same genotype but fed the control diet. #P<0.05, compared with mice fed with the same diet but with the $ApoE^{-/-}$ genotype. The numbers below each column are the number of mice used in the experiments. (C) Representative images of Oil Red O–stained sections of aortic sinus regions from mice of the designated genotype and food groups. Scale bar, 0.2 mm. (D) The lesions in the aortic sinus region were quantified as the percentage of the total lumenal area of aortas. *P<0.05, compared with mice with the same genotype but fed the control diet, n≥4. There were no detectable lesions formed in the aortic sinus regions of $ApoE^{+/+}$ mice. (E) Representative images of calcification in the aortas and lesions as determined with Von Kossa staining (purple; indicated by black arrows). Scale bar, 0.2 mm. (F) The area containing calcification deposition was measured as a percentage of the total lumenal cross-sectional area of aortas. *P<0.05, compared with mice fed the same diet but with the $ApoE^{-/-}$ genotype, n≥5. No detectable calcification detected in aortas of $ApoE^{+/+}$ mice.

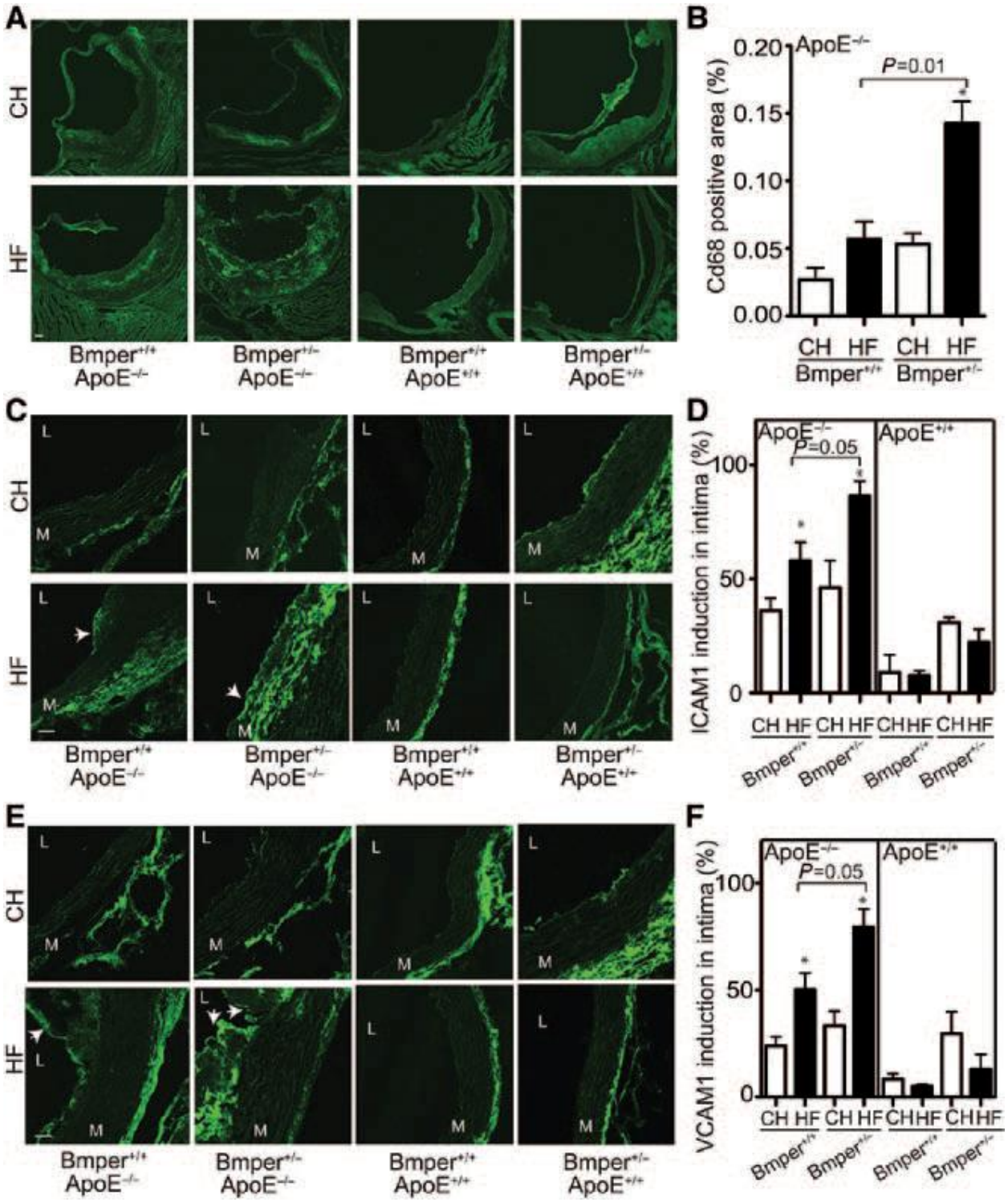

Figure 2-2. BMPER haploinsufficiency increases macrophage infiltration and intimal inflammation in ApoE−/− mice.

Representative images showing the CD68-labeled macrophages infiltrate in atherosclerotic lesions of mice of the designated genotype and food group. Scale bars, 100 μm. (B) Macrophage infiltration was

quantified by measuring the area of CD68-positive cells and calculating this as a percentage of the total vessel area of aorta studied. *P<0.05, compared with mice of the same genotype but fed the control diet. n=3. (C–F) Intracellular adhesion molecule 1 (ICAM1) (green in C) and vascular cell adhesion molecule 1 (VCAM1) (green in E) immunofluorescence in aortic lesions of mice of the designated genotype and food group. Shown are representative images of 3 to 5 mice. Scale bars, 25 μm. Arrows indicate plaques. (D and F) The intimal length containing ICAM1 (C) and VCAM1 (E) was measured as a percentage of the total intimal conference. *P<0.05, compared with mice of the same genotype but fed the control diet, n≥3. L indicates lumen; M, media.

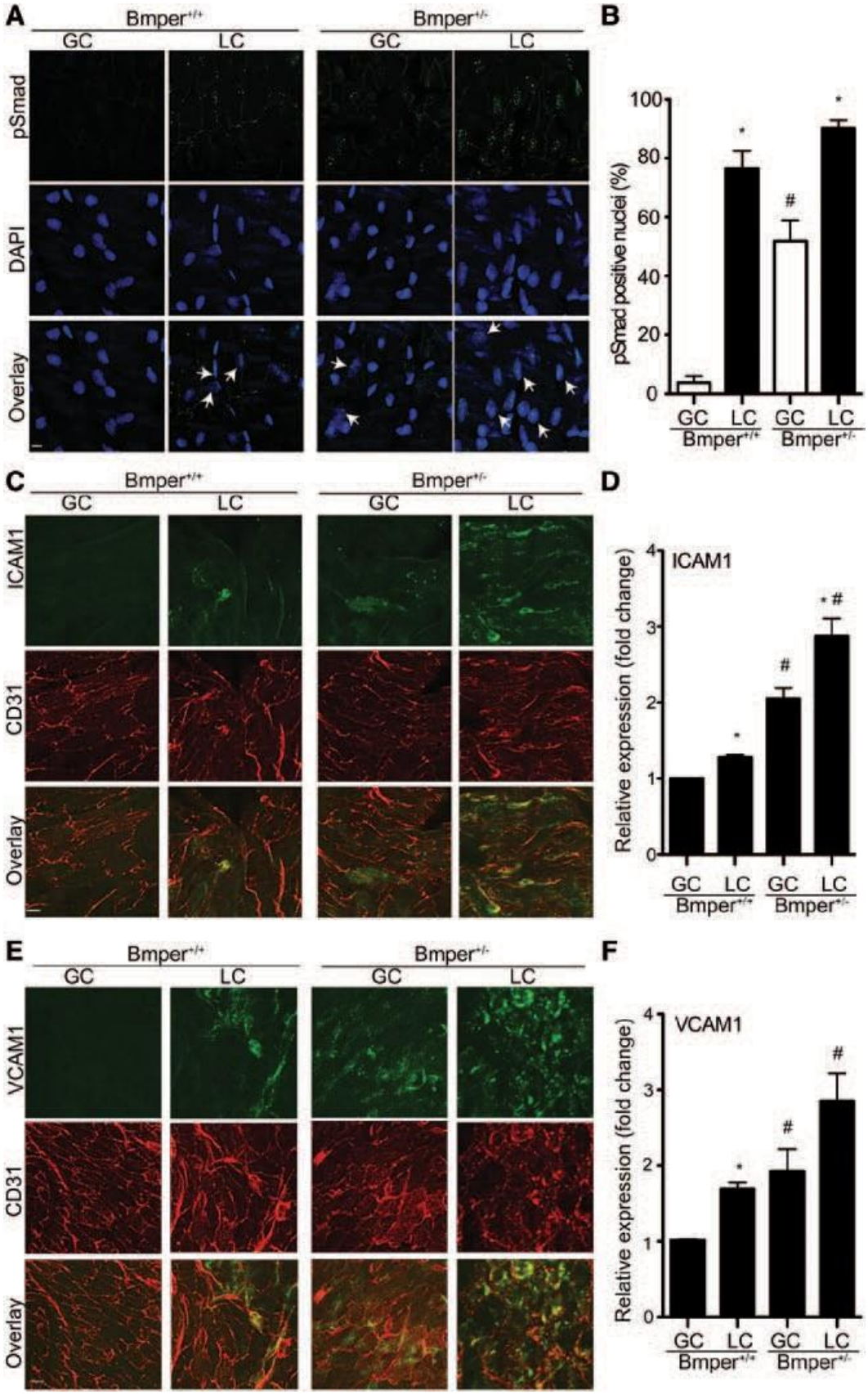
A
Bmper+/+
Bmper+/-
GC
LC
pSmad
DAPI
Overlay
B
pSmad positive nuclei (%)
100
80
60
40
20
0
GC LC GC LC
Bmper+/+ Bmper+/-
C
ICAM1
CD31
Overlay
D
ICAM1
Relative expression (fold change)
4
3
2
1
0
E
VCAM1
CD31
Overlay
F
VCAM1
Relative expression (fold change)

Figure 2-3. BMPER haploinsufficiency results in increased BMP activity and expression of inflammatory adhesion molecules in the ApoE+/+ endothelium of the greater curvature (GC) and lesser curvature (LC) of the aortic arch.
(A) *En face* staining of the GC and LC in the aortic arch of $BMPER^{+/-}$ and $BMPER^{+/-}$ mice was performed using an antibody specific for phosphorylated Smad (pSmad) 1, 5, and 8 (green). Nuclei were counterstained with DAPI (blue). Arrows indicate pSmad positive nuclei. Scale bar, 10 μm. (B) pSmad positive nuclei were quantified as a percentage of all nuclei per field. *P<0.05 compared with pSmad positive nuclei (%) in the GC region of the same mice; #P<0.05 compared with pSmad positive nuclei (%) in the same region of wild-type littermates, n=3. (C–F) *En face* staining was performed for intracellular adhesion molecule 1 (ICAM1) (green in C) and vascular cell adhesion molecule 1 (VCAM1) (green in E) and the endothelial marker CD31 (red in C and E). Scale bar, 10 μm. (D and F) the average intensity of ICAM1 (D) and VCAM1 (F) was measured as fold change over the level of intensity in the GC of wild-type mice. *P<0.05 compared with the relative expression level in the GC of the same mice; #P<0.05 compared with the relative expression level in the same region of wild-type littermates, n=3.

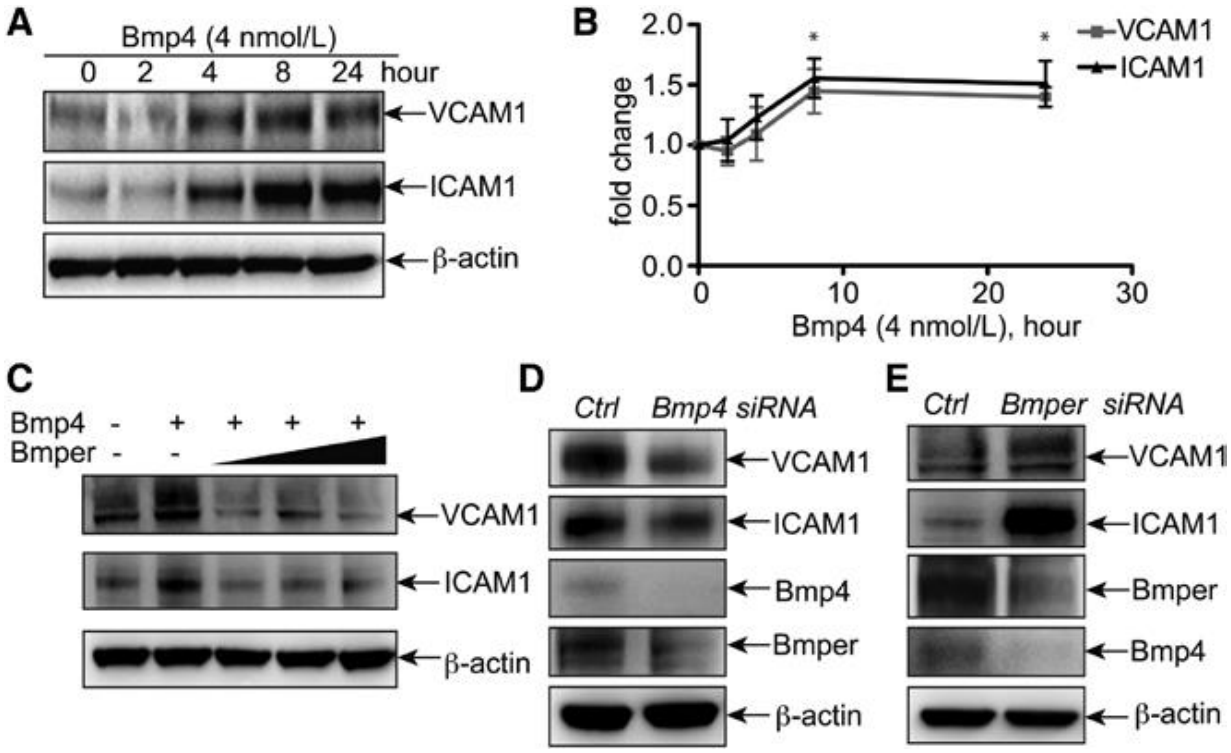

Figure 2-4. BMPER inhibits BMP4– induced ICAM1 and VCAM1 expression.
Human umbilical vein endothelial cells (HUVECs) were treated with 4 nmol/L of BMP4 for different time periods as indicated and then cell lysates were subjected to Western blotting with specific antibodies against ICAM1 and VCAM1. (B) ICAM1 and VCAM1 band intensity was quantified with ImageJ and normalized against the actin level. *P<0.05 compared with the sample without BMP4 treatment, n=3. (C) HUVECs were treated with 4 nmol/L BMP4 and increasing concentrations of BMPER (5, 10, and 20 nmol/L) for 8 hours. Cell lysates were then subjected to Western blotting with specific antibodies against ICAM1 and VCAM1. (D) HUVECs were transfected with BMP4 small interfering RNA (siRNA) or control siRNA. Cells were harvested 18 hours later and subjected to Western blotting. (E) HUVECs were transfected with BMPER siRNAs or control siRNA. Cells were harvested after 96 hours and subjected to Western blotting.

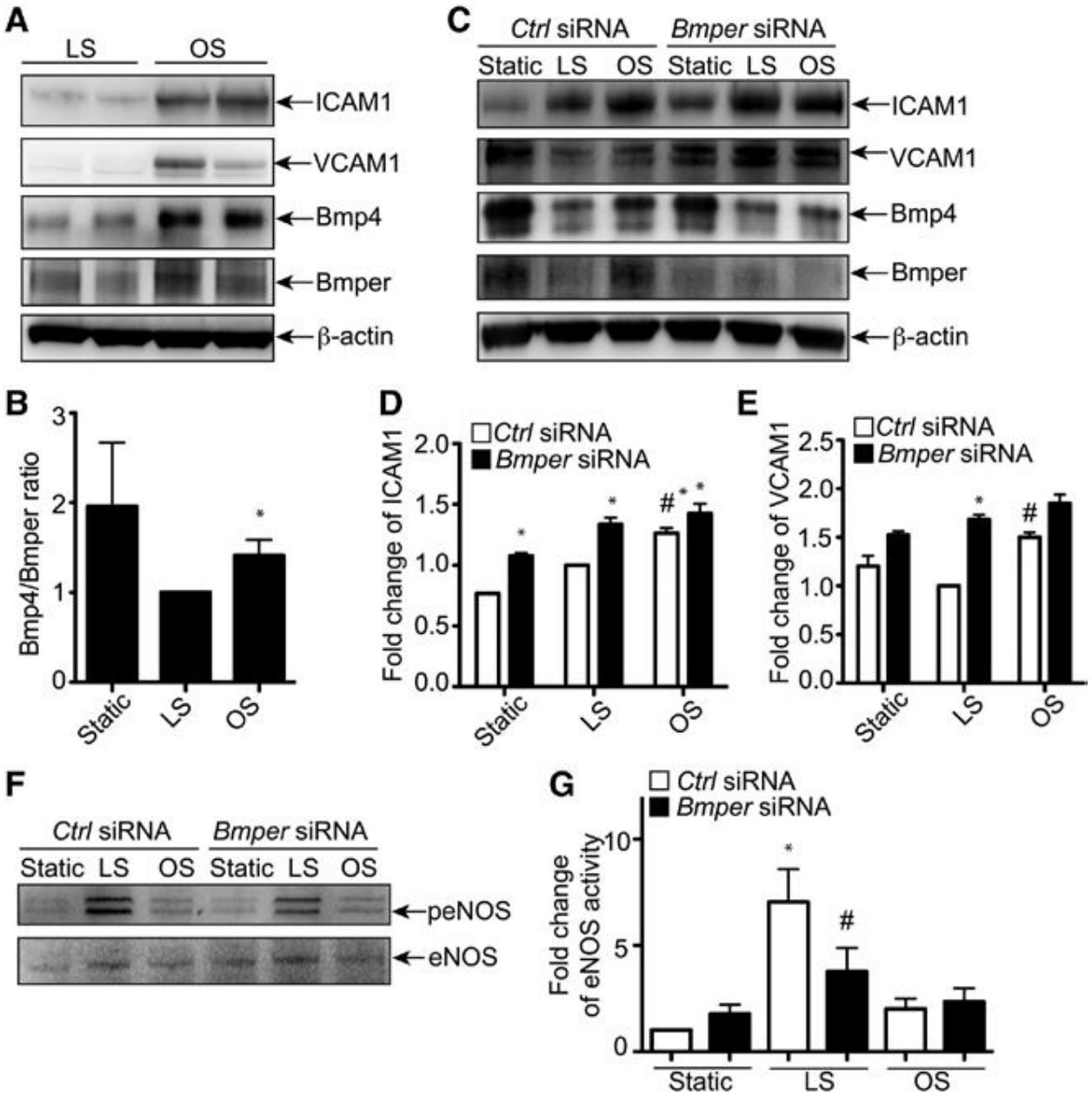

Figure 2-5. BMPER is required for the regulation of ICAM1 and VCAM1 expression by fluid shear stress.

A) Human umbilical vein endothelial cells (HUVECs) were subjected to oscillatory shear stress (OS, ± 5 dyn/cm^2) or laminar shear stress (LS, 20 dyn/cm^2) or remained static in the incubator for 8 hours. Cell lysates were used for immun0-blotting to detect the expression of BMPER and BMP4 and the induction of inflammatory adhesion molecules ICAM1 and VCAM1. (B) The band intensity of BMP4 and BMPER (A) was quantified with ImageJ and is presented as the ratio of BMP4/BMPER protein level compared with the LS condition. *P<0.05 compared with the cells exposed to laminar shear stress, n=4. C, HUVECs were transfected with BMPER or control (small interfering RNAs) siRNAs. Four days later, cells were exposed to OS (± 5 dyn/cm^2), LS (20 dyn/cm^2), or static conditions for 8 hours. (D and E) The band intensity of ICAM1 (D) and VCAM1 (E) was quantified with ImageJ and is presented as the relative fold change of protein level compared with the LS condition. *P<0.05 compared to the cells transfected with control siRNAs, n=3; #P<0.05 compared

with the cells exposed to LS, n=3. (F) HUVECs were transfected with BMPER or control siRNAs. Four days later, cells were exposed to OS (± 5 dyn/cm^2), LS (20 dyn/cm^2), or static conditions for 8 hours. Cell lysates were used for immuno -blotting with phospho–endothelial nitric oxide synthase (eNOS) (Ser1177) and eNOS antibodies. (G) The band intensity of phospho-eNOS (Ser1177) (E) was quantified with ImageJ and is presented as the relative fold change of protein level compared with the total eNOS protein level. *P<0.02 compared with the cells at the static condition; #P<0.03 compared with the cells transfected with control siRNA, n=3.

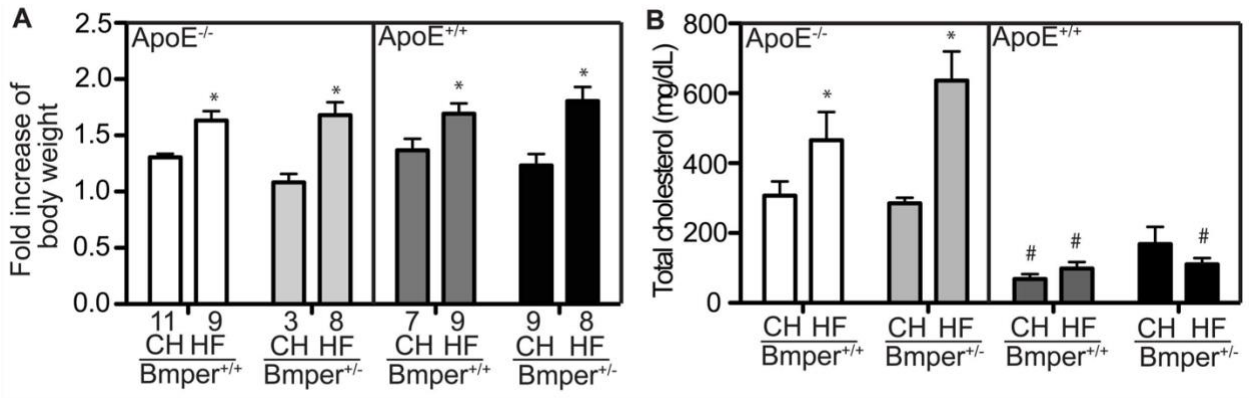

Figure 2-6. The changes in body weight and total cholesterol level of BMPER/ApoE mice after 20 weeks on standard chow (CH) or high fat diet (HF).

A. The change in body weight after 20 weeks was calculated and demonstrated as a fold-change of body weight at Week 20 over Week 0. The numbers listed below the graph are the number of mice used for this experiment. (B) The total serum cholesterol level was measured at week 20. *, $P<0.05$, compared to mice with the same genotype but fed with the control diet. #, $P<0.05$, compared to mice fed with the same diet but with the $ApoE^{-/-}$ genotype.

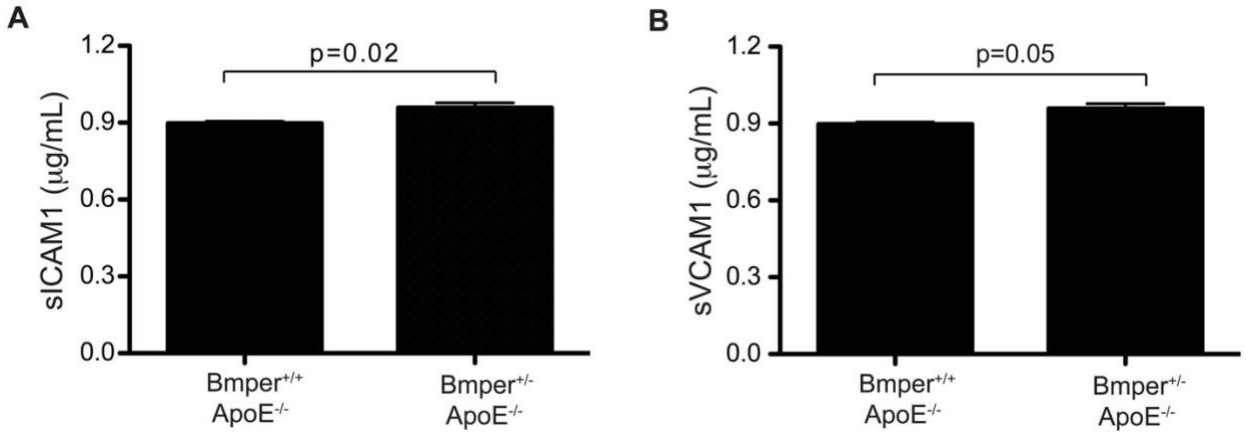

Figure 2-7. sICAM1 and sVCAM1 plasma levels increased in BMPER+/- mice after 4 weeks consuming the high fat diet.

Blood was collected, and the protein levels of soluble ICAM1 (A) and VCAM1 (B) were measured at 2eek 4. n=3.

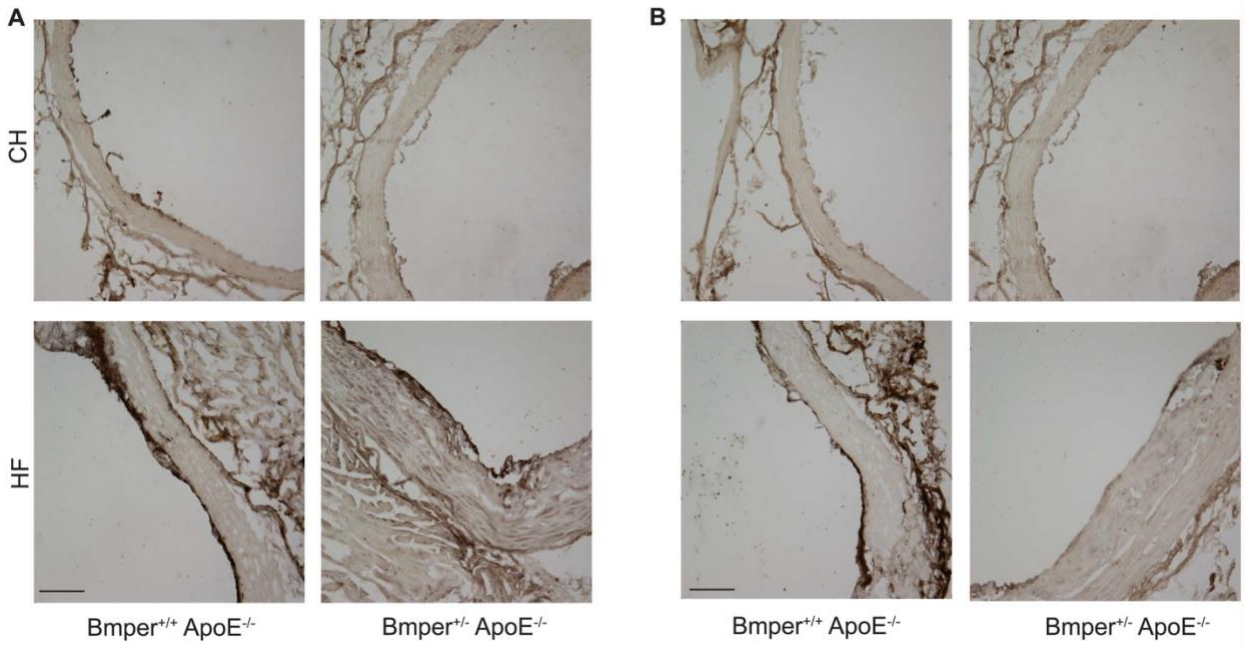

Figure 2-8. BMPER and BMP4 expression was increased in mice fed a high fat diet.
The cryo-sections of aortic root were stained with anti-BMPER (A) and anti-BMP4 (B) antibodies. All the mice were on the ApoE-/- background. Scale bar: 200 μm.

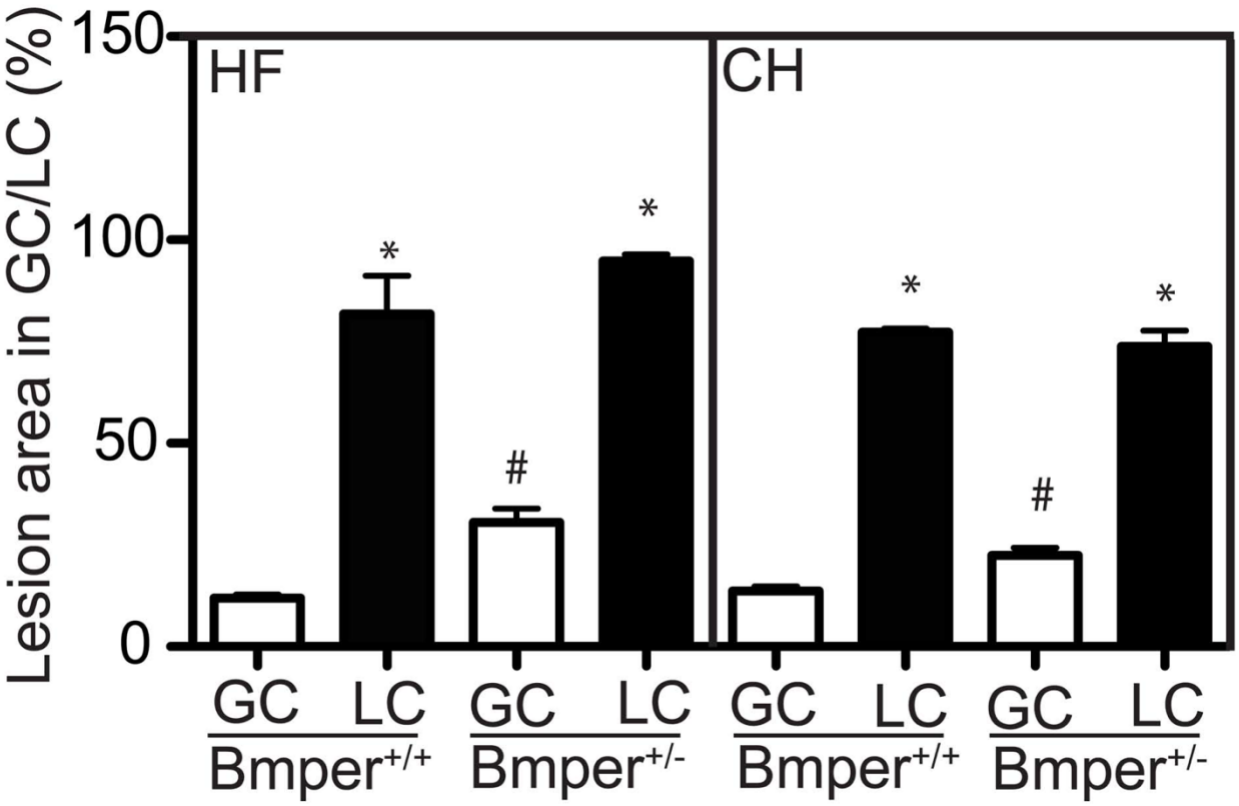

Figure 2-9. 9 BMPER haploinsufficiency leads to aggravated atherosclerotic plaque formation in aortic arch area.

Mice were fed a high fat diet (HF) or standard chow (CH) for twenty weeks. The aortas were dissected out and stained with Oil Red O. The lesions on the surface of each greater and lesser curvature of aorta arch were quantified as a percentage of the total area of GC and LC. *, $P<0.002$, compared to that lesions located in GC of the same mouse. #, $P<0.05$, compared to $BMPER^{+/+}$ mice fed with the same diet. All the mice were on the $ApoE^{-/-}$ background.

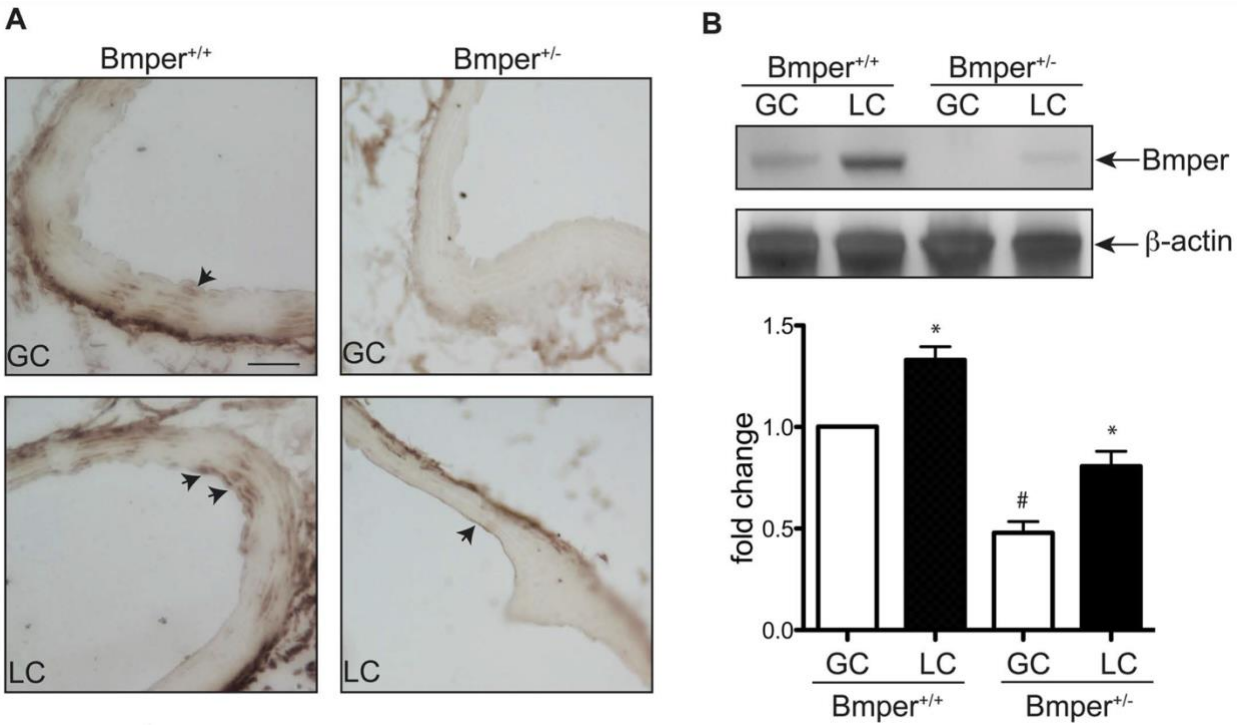

Figure 2-10. BMPER protein level was increased in the LC compared to GC.
(A) The regions of GC and LC located in aortic arch of mouse aortas were processed for staining with BMPER antibody. Scale bar, 200 μm. The arrows represent the positive staining of BMPER protein. Scale bar: 200 μm. (B) The vessel lysates obtained from the GC and LC region of mice were subjected to the immuno-blotting with BMPER antibody. Each sample was obtained from two mice. *, $P<0.05$, compared to the sample of the GC in the same mouse. #, $P<0.05$, compared to the GC region of $BMPER^{+/+}$ mice. n=3.

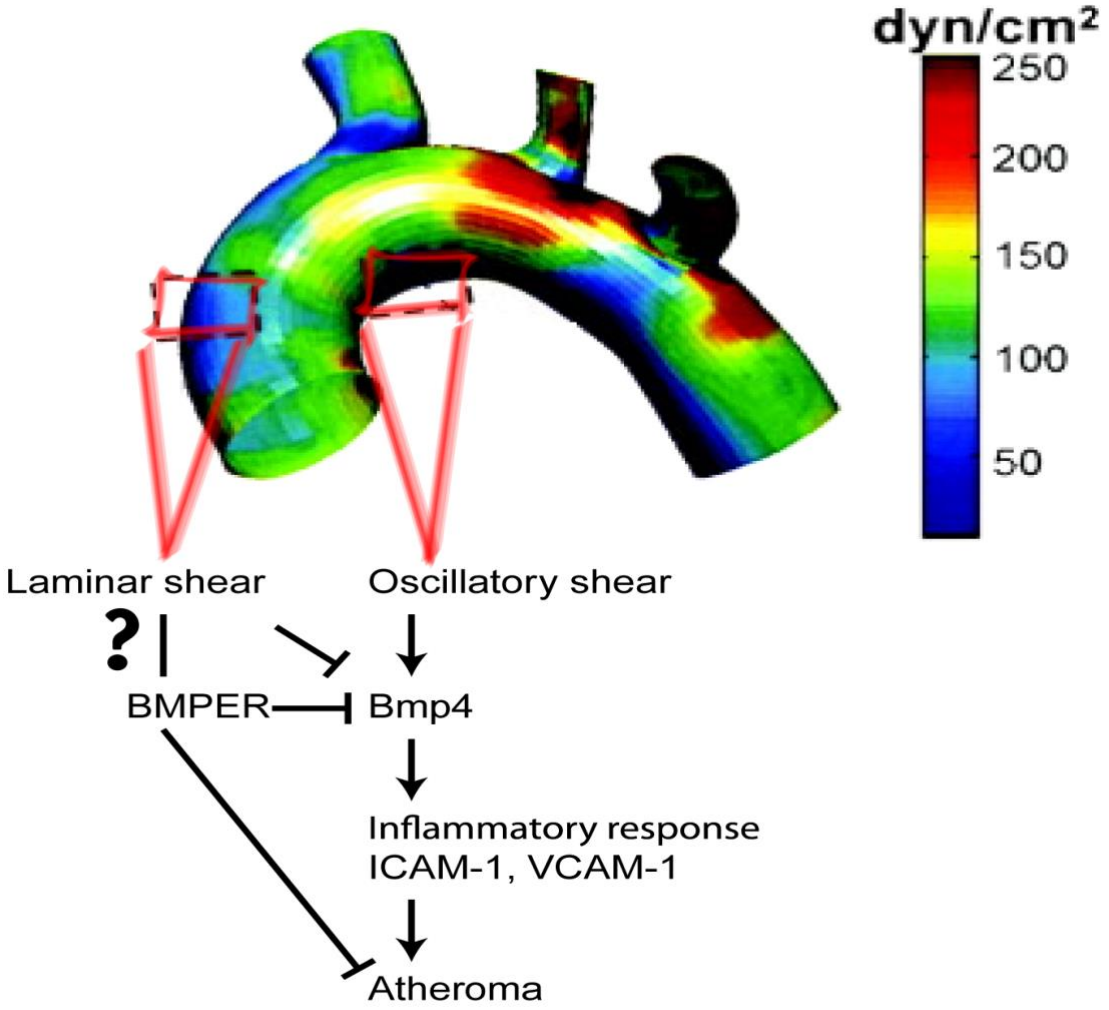

Figure 2-11. Schematic illustration demonstrating how BMPER exerts protective effects in the vasculature by regulating BMP4 signaling.

CHAPTER 3: LRP1-DEPENDENT BMPER SIGNALING REGULATES LPS-INDUCED ACUTE VASCULAR INFLAMMATION

3.1 INTRODUCTION

Sepsis is a common cause of significant morbidity and mortality worldwide. It is the tenth leading cause of overall death in the United States, and the incidence of sepsis is 750,000 and costs $17 billion dollars annually creating a major healthcare burden.[25–27] Despite being one of the oldest clinical syndromes in medicine, there is no specific or targeted therapy and the number of patients has continued to increase by 9% each year over the past two decades.[25] Treatment has been constrained to the useage of antibiotics and supportive care. This underscores the fact that fundamental gaps remain in our knowledge of the pathiophysiological mechanisms that drive sepsis. Injury and dysfunction of multiple organs are a clinical manifestation of sepsis, with the lung most commonly involved. Sepsis often leads to ALI or its more severe form, ARDS whose distinguishing features are impairment of pulmonary vascular integrity and endothelial dysfunction. The bacterial endotoxin, lipopolysaccharide (LPS), is one of the leading contributing factors to ALI in sepsis.

The endothelium is a major target of sepsis, and endothelial dysfunction accounts for significant amount of the pathology in sepsis. In response to LPS in the blood, endothelial cells act as the first line of defense by recognizing invading pathogens via pattern recognition receptors (PRR) and initiating inflammatory and coagulation cascades. Proinflammatory cytokines secreted from endothelial cells further activate neutrophils, monocytes, tissue macrophages and/or endothelial cells. Endothelial cell activation induced by LPS will

eventually result in increased vascular permeability, allowing increased flux of proteins, fluid and immune cells across vessels into tissues. However, the underlying mechanisms mediating endothelial activation in response to LPS remain largely unknown.

Toll-like receptor 4 (TLR4) has been recognized as the major receptor for LPS. Ligation of LPS to TLR4 activates NFκB and nuclear factor of activated T cells (NFAT) pathways. In human umbilical vein endothelial cells (HUVECs), TLR4, MyD88 and Mal/TIRAP adaptor proteins are required for the activation of NFκB and production of interleukin-6 (IL-6).[28] Animal studies with inactive NFκB signaling indicate that, in response to LPS-induced endotoxemia, NFκB activation acts as a quick adaptive response, which provides an important survival signal and maintains a normal but dynamic endothelial barrier function.[29] On the other hand, LPS activates transcriptional factor NFAT in endothelial cells, which results in increased expression of pro-inflammatory cytokines such as IFN-γ and TNFα.[30] The activation of NFAT is mediated by reactive oxygen species (ROS)-driven Ca2+ signaling pathway and TLR4 may be required for ROS generation.[30] In activated immune cells such as dendritic cells, CD14 is another receptor of LPS leading to NFAT activation, likely through Src-family kinase and phospholipase Cγ2, and Ca2+/calcineurin signaling.[31] In endothelial cells, CD14 has also been suggested to function together with TLR4 to mediate LPS-induced E-selectin and IL-6 production.[32] Although the exact roles of TLR4 and CD14 in LPS-mediated NFAT activation and endothelial inflammatory responses remain to be further clarified, NFAT activation is recognized as a crucial transcription factor controlling the expression of pro-inflammatory cytokines.

Endothelial integrity and vascular homeostasis are tightly regulated by multiple signaling pathways such as bone morphogenetic protein (BMP) signaling.[33] BMP-binding endothelial regulator (BMPER), an extracellular regulator of BMPs,[13,21] has been identified as an important regulator of vascular inflammation and atherosclerosis.[18,19,34] Knockdown of BMPER by its specific siRNA or its deficiency in BMPER+/- mice potentiates TNFα induced endothelial inflammatory responses.[19] This anti-inflammatory phenotype of BMPER

is mediated by blocking BMP activity, which likely explains the atheroprotective function of BMPER.[34] However, it is not clear whether BMPER regulates inflammatory responses in endothelial cells in an acute setting, such as LPS challenge. We have recently demonstrated that LDLR-related protein (LRP) 1, a member of the LDL receptor family, binds with BMPER at the cell membrane, the complex is endocytosed and has been shown to regulate angiogenesis during zebrafish vein development.[35] The mature form of LRP1 is a heterodimer composed of a 515-kDa α chain (LRP1α), possessing four extracellular ligand binding domains, and an 85-kDa membrane-anchored cytoplasmic β chain (LRP1β), which remains non-covalently associated with α chain. LRP1 is an endocytic receptor for multiple signaling pathways and mediates their signals through its β chain, which interacts with many scaffolding proteins.[36–42] In addition, processed forms of LRP1β can also translocate into nucleus and regulate the enzyme activity of PARP1[43] and expression of PPAR target genes by acting as a PPARγ co-activator.[44] Although LRP1 is required for the endocytosis of BMPER signaling complex in endothelial cells, it remains elusive whether the coupling of BMPER to LRP1 may also initiate their own signaling events.

BMPER null mice die at birth.[13] In this study, we used BMPER haploinsufficient mice to study the effect of reduced BMPER expression on LPS-induced endothelial inflammation. Surprisingly, we observed that $BMPER^{+/-}$ mice exhibit reduced vascular inflammatory responses upon LPS treatment as shown by several parameters, including endothelial permeability, pulmonary edema, survival rate and production of pro-inflammatory cytokines. Interestingly, BMPER activates NFATc1 in a LRP1-dependent but BMP-independent manner. Furthermore, the coordinative actions of LRP1/NF45 nuclear export and NFATc1 nuclear import may play a crucial role for BMPER-induced NFATc1 activation. These results indicate that inhibition of BMPER signaling limits endotoxemia-induced pulmonary inflammatory responses and that the BMPER/LRP1 signaling axis may provide potential therapeutic targets against sepsis-induced acute lung injury.

3.2 RESULTS

3.2.1 LPS-INDUCED LUNG INJURY AND MORTALITY IS REDUCED IN BMPER$^{+/-}$ MICE

BMPER has been well characterized in the setting of chronic inflammation and atherosclerosis and established as a protective mediator of these processes by inhibiting BMP activity in the endothelium.[18,19,34] However, it is unknown how BMPER regulates vascular responses during acute inflammation. We used a LPS-induced model of endotoxemia and BMPER$^{+/-}$ mice (BMPER$^{-/-}$ mice die at birth.[13]) to investigate the *in vivo* role of BMPER in acute inflammation of the endothelium. We first challenged BMPER$^{+/-}$ mice and their littermate controls (BMPER$^{+/+}$ mice) with a lethal dose of LPS (15 mg/kg i.v.). We were surprised to discover all BMPER$^{+/+}$ mice died within 2 days while the majority of BMPER$^{+/-}$ mice recovered with a 7-day survival rate at approximately 62.5 percent (Figure 3.1A). Next we evaluated histopathological changes in the lungs of BMPER$^{+/-}$ and BMPER$^{+/+}$ mice 12 hours after a sub-lethal dose of LPS (10 mg/kg i.v.). We observed an increased number of inflammatory cells in the interstitum and alveolar space, proteinacous debris in the alveolar space, interalveolar septal thickening and interstitial edema in BMPER$^{+/+}$ mice (Figure 3.1B), while BMPER$^{+/-}$ mice exhibited much lower instances of these indices of lung injury and had a much reduced lung injury score (Figure 3.1C). These data suggest that BMPER haploinsufficiency protects against endotoxemia-induced pulmonary injury.

3.2.2 LPS-INDUCED ENDOTHELIAL PERMEABILITY IS LESS SEVERE IN BMPER HAPLOINSUFFICIENT MICE

To extend our in vivo analysis, we next compared the several lung injury-associated parameters of endothelial dysfunction, pulmonary edema and BALF protein concentration. When BMPER$^{+/+}$ control mice were challenged with a sub-lethal dose of LPS (10 mg/kg i.v.), they rapidly developed symptoms consistent with sepsis (e.g., lethargy, ocular discharge; data not shown), while BMPER haploinsufficient mice (BMPER$^{+/-}$) demonstrated less severe symptoms. Extravasation of Evans blue dye (EBD) from circulation into the lung tissue and elevated protein content in the alveolar space are often used as an indicators of

elevated capillary permeability. We observed that extravasated EBD content in the lung tissue of BMPER$^{+/-}$ mice was significantly less than that from BMPER$^{+/+}$ mice (Figure 3.2A,B) as well as total protein collected from broncioalveolar lavage fluid (BALF). Similarly the lung wet/dry weight ratio, a measure of pulmonary edema, and the total protein concentration in the BALF of BMPER$^{+/-}$ mice, following LPS injection was significantly smaller than that of BMPER$^{+/+}$ mice (Figure 3.2C, D). Taken together, these data suggest that BMPER haploinsufficiency protects against pathological endothelial pulmonary permeability.

3.2.3 LPS-induced Pro-inflammatory Cytokine Production and Leukocyte Migration are attenuated in BMPER$^{+/-}$ mice

Endotoxemia-induced lung inflammation is associated with increases in the production of cytokines, both systemically and in the alveolar compartment, and leukocyte infiltration into target tissues. Therefore, we evaluated the concentration of LPS-induced pro-inflammatory cytokines in the serum of BMPER$^{+/+}$ and BMPER$^{+/-}$ mice. IFNγ, IL-6 and TNF-α were induced in BMPER$^{+/+}$ mice by LPS, while BMPER$^{+/-}$ mice had a significantly lower response (Figure 3.3A-C). To further assess the influence of BMPER haploinsufficiency on pulmonary inflammation, we determined in the BALF several parameters of lung inflammation, including cell infiltration, myeloperoxidase (MPO) activity and the levels of IFNγ, IL-6 and TNF-α. In response to LPS, both BMPER$^{+/+}$ and BMPER$^{+/-}$ mice had increased leukocyte infiltration in the BALF, but the cell count in BALF of BMPER$^{+/-}$ mice was significantly fewer than those in BMPER$^{+/+}$ mice (Figure 3.4A). Similarly, myeloperoxidase (MPO) activity was also dramatically lower in BMPER$^{+/-}$ mice, compared to BMPER$^{+/+}$ mice (Figure 3.4B) suggesting that BMPER haploinsufficiency inhibits leukocyte infiltration into the alveolar space. Next, we measured cytokine levels in BALF and found that the individual levels of IFNγ, IL-6 and TNF-α were significantly decreased in BMPER$^{+/-}$ mice (Figure 3.3D-F). Taken together, BMPER$^{+/-}$ mice demonstrate a

blunted acute pulmonary inflammatory response upon LPS challenge, having reductions in leukocyte infiltration and pro-inflammatory cytokine production.

3.2.4 BMPER REGULATES NFATC1 SIGNALING

The inhibitory effect of lower gene dosage on LPS-induced lung injury in BMPER haploinsufficient mice was unexpected because of the known anti-inflammatory role of BMPER in chronic inflammatory responses. The preceeding data suggest BMPER might regulate acute and chronic inflammatory responses through distinct pathways. To understand the underlying molecular mechanisms responsible for BMPER's action, we performed gene profiling analysis with BMPER treated endothelial cells and searched for changes in gene expression. Microarray analysis of endothelial cells treated with BMPER or control revealed that BMPER elicits either up-regulation or down-regulation of genes that are not associated with BMP transcriptional regulation (Figure 3.5A). To further examine these observations, we used TRANSFAC analysis to map transcription factor binding sites upstream of the identified BMP-independent BMPER-regulated genes. Interestingly, we found that a number of genes regulated by BMPER contain NFAT consensus binding sites including phospholipase Cβ1 and NFATc1, which itself is a member of NFAT transcription factors. Immunostaining showed the translocation of NFAT to the nucleus after BMPER treatment confirming the activation of NFAT by BMPER (Figure 3.5B). There are mainly five members of NFAT transcriptional factors that are evolutionarily related to the REL- NFkB family of transcription factors: NFAT1 (also known as NFATc2 or NFATp), NFAT2 (also known as NFATc1 or NFATc), NFAT3 (also known as NFATc4), NFAT4 (also known as NFATc3 or NFATx) and NFAT5 (also known as tonicity enhancer binding protein; TonEBP). To examine the relationship between BMPER and NFAT, we assessed the induction of NFATs in response to BMPER treatment. By performing real-time PCR analysis, we demonstrated that NFATc1 was the most induced NFAT in response to BMPER treatment, with the peak at one hour (Figure 3.5C).

BMPER plays a role in LPS signaling pathway in endothelial cells. By using mouse lung endothelial cells (MLECs), we investigated whether NFAT, an important transcription factor of LPS-induced acute inflammatory responses in endothelial cells,[30,31,45,46] can be regulated by BMPER. As expected, LPS increased NFAT activity as measured by NFAT reporter luciferase activity (Figure 3.6A; data provided by Dr. Hua Mao). However, when BMPER expression in MLECs was knocked down with its specific siRNA (Figure 3.6E; data provided by Dr. Hua Mao), we observed a ~two-fold decrease in NFAT activation, compared to control MLECs (Figure 3.6A; data provided by Dr. Hua Mao). These data suggest that BMPER is required for NFAT activation in response to LPS. Next, we tested whether BMPER could activate NFAT by performing the NFAT reporter assay in endothelial cells in response to BMPER. When mouse lung endothelial cells were treated with BMPER, we observed an increase in NFAT transcriptional activity (Figure 3.6B). NFATc1 must to be dephosphorylated then translocate from cytoplasm to the nucleus for activation. We performed fractionation assays to determine whether subcellular localization of NFATc1 can be regulated by BMPER. Indeed, we observed an increase of NFATc1 accumulation in the nucleus after BMPER treatment for 15 to 60 minutes (Figure 3.6C, D). Immunostaining also confirmed NFAT nuclear translocation in response to BMPER in endothelial cells (Figure 3.5B). Taken together, these data suggest BMPER is not only necessary but also sufficient for NFATc1 activation.

3.2.5 LRP1 MEDIATES NFAT ACTIVATION INDUCED BY BMPER

To determine how BMPER activates NFATc1, inhibitors of different signaling pathways were used to dissect downstream signaling pathways. Importantly, we showed that cyclosporin A (CsA; calcineurin inhibitor) and U0126 (MEK1/ERK inhibitor) blocked the activation of NFAT upon BMPER treatment (Figure 3.7A). However, Smad6, which is the inhibitor of the BMP's downstream signaling mediators Smad1, 5 and 8, failed to inhibit NFAT activation (Figure 3.7A), suggesting that BMPER activates NFAT through BMP

independent pathways. We have recently demonstrated that LRP1 is associated with BMPER and is required for BMPER's regulatory effects on angiogenesis.[35] Given that the intracellular domain of LRP1β contains multiple serine, threonine and tyrosine residues that can be phosphorylated by PKA or Src,[42,47] we hypothesized that BMPER may initiate signaling cascades directly through LRP1. Treatment with BMPER at increased dosages promoted ERK activation. However, ERK activation induced by BMPER was not inhibited by BMP4 neutralizing antibody (Figure 3.7B), suggesting that BMPER may induce ERK activation in a BMP4-independent manner. On the other hand, LRP1 knockdown dramatically decreased ERK activation upon BMPER treatment in MLECs that have been transiently transfected with LRP1 siRNA or mouse endothelial cells stably transfected with LRP1 shRNA (EC50 is 51.20 nM; Figure 3.7C,D), suggesting that LRP1 is required for BMPER-induced ERK activation. Given that ERK pathway is required for BMPER-induced NFAT activation, we then tested whether LRP1 is required for NFAT activation. Indeed, LRP1 knockdown significantly inhibited NFAT reporter activity in response to BMPER in MLECs (Figure 3.7E, **Dr. Hua Mao). These results suggest that ERK activation mediated by LRP1 and calcium dependent calcineurin pathways are required for NFAT activation upon BMPER treatment.

However, many NFAT regulatory elements can also be regulated by NFκB. For example, CD28 response element of the IL-2 promoter contains a dimeric NFAT/NFκB site, which may bind both NFAT and NFκB and function cooperatively with AP-1 protein that is associated with the adjacent AP-1 site.[48,49] Therefore, we tested whether BMPER could also mediate NFκB signaling. After LPS treatment, we observed a more than two-fold increase in IKK activation in BMPER siRNA silenced MLECs, compared to control MLECs (Figure 3.8A,B). These data suggest that BMPER is required for IKK activation in response to LPS. Next, we investigated whether BMPER itself is sufficient to activate IKK and initiate acute inflammatory response. BMPER treatment induces a significant increase in IKK activation following 15 and 60 minutes of BMPER treatment (Figure 3.8C,D). Additionally, NFκB

transcriptional activity was increased, determined by NFκB reporter assays (Figure 3.8G). However, LRP1 knockdown by its specific siRNA decreased BMPER-induced NFκB activity. Taken together, these data suggest that BMPER/LRP1 axis can also activate NFκB transcriptional activity.

3.2.6 NF45 IS ASSOCIATED WITH LRP1B AND INVOLVED IN NFAT ACTIVATION

LRP1's α chain (LRP1α) is responsible for extracellular ligand binding and its β chain (LRP1β) for transducing signals. Additionally, LRP1β can be further processed[50] and translocated to nucleus, where it interacts with nuclear proteins such as poly(ADPribose) polymerase-1 (PARP-1)[43] and PPARγ[44] to regulate cell cycle progression and gene transcription. Because we have demonstrated that LRP1 is required for BMPER-induced ERK activation (Figure 3.7D), we wanted to determine if the nuclear LRP1β fragment might play a role in BMPER-induced NFAT activation. To address this question, we searched for LRP1β-interacting proteins as shown in our previous publication.[43] First, we performed liquid chromatography associated mass spectrometry (LC-MS/MS) analysis to identify LRP1β-associated proteins in HEK 293 cells (Figure 3.9A). Nuclear factor 45/interleukin binding factor 2 (NF45/ILF2) was among proteins that co-immunoprecipitated with Flag-LRP1β (Figure 3.9A). NF45 is a nucleic acid-binding protein that regulates cellular gene expressions involved in DNA metabolism, transcription, translation, RNA export and microRNA biogenesis.[51–56] In addition, NF45 is considered as a transcriptional activator of IL-2 gene.[56] Previous reports show that NF45 and NFAT bind to the same promoter region of IL-2 promoter. However, they have different consensus binding sequences (TGTTTAC for NF45 and TGGAAAAT for NFAT).[57] NF45, unlike NFAT, is associated with the IL-2 ARRE-2 site even at basal condition.[57] To date, it remains unknown whether this interchangeable binding of NF45 and NFAT transcriptional complex is important for IL-2 transcriptional activation. To study the role of NF45 in BMPER-induced gene expression, we first confirmed the interaction between overexpressed Flag-LRP1β and NF45 in HEK 293

cells (Figure 3.9B). Moreover, their endogenous association was detected in MLECs and blocked by the inhibitors of PKA- PKI, Src (PP2) or their combined treatments (Figure 3.9C, F), suggesting that the interaction of LRP1β with NF45 requires LRP1β phosphorylation by PKA and Src. Furthermore, both immunofluorescence imaging and subcellular fractionation analysis demonstrated that LRP1β and its processed intracellular domain, and NF45 were co-localized mainly in the nucleus of MLECs at basal condition (Figure 3.9D,E). Surprisingly, cytosolic levels of NF45, LRP1β and its intracellular domain, but not the processed form of LRP1β at 25 kDa, were increased in response to BMPER treatment (Figure 3.9E), suggesting that BMPER induces the cytosol translocation of NF45, LRP1β and its intracellular domain, but not the LRP1 processing. To further test whether NF45 translocation takes place in LPS-induced inflammatory setting, we performed immunofluorescent studies in MLECs and lung sections. In LPS-treated MLECs, NF45 positive signals in the cytosol fraction were significantly increased (Figure 3.10A,B ***Data by Dr. Hua Mao). However, the increased signals were blocked in BMPER siRNA transfected MLECs. Additionally, 70.6% of NF45 signals were localized in cytosol of pulmonary vascular cells in $BMPER^{+/+}$ mice upon LPS injection (Figure 3.10 C,D ***Data by Dr. Hua Mao). However, the cytosol-localized NF45 signals were decreased to 55.1% in $BMPER^{+/-}$ mice. Together these results indicate that NF45 was translocated from the nucleus to cytoplasm in response to LPS and its translocation was inhibited by BMPER deficiency, supporting the hypothesis that NF45 nuclear export is regulated by LPS through a BMPER-dependent pathway.

Taken together, our results indicate that BMPER acts as a pro-inflammatory stimulus during acute lung injury. Its action requires coordination of multiple signaling cascades, including the calcium-dependent calcineurin and LRP1-dependent ERK activation pathways, the cytosolic translocation of NF45 and nuclear translocation of NFATc1, which eventually lead to the activation of NFATc1 and induction of its downstream inflammatory target genes. Our studies suggest BMPER signaling is a potential therapeutic target to prevent sepsis-induced pulmonary inflammation and injury.

3.3 DISCUSSION

The roles of BMPER in inflammation have been examined in several mouse models of inflammation including thioglycollate-induced peritonitis and high fat diet induced atherosclerosis.[19,34] The studies suggest that BMPER plays an anti-inflammatory role through modulating BMP activity and thereby blocking TNF-α or oscillatory shear-mediated induction of adhesion molecules such as ICAM-1 and VCAM1. In this study, we have demonstrated for the first time a pro-inflammatory role of BMPER in LPS-induced acute lung injury. $BMPER^{+/-}$ mice exhibit reduced responses upon LPS challenge. Our biochemical studies suggest BMPER regulates inflammatory responses through the NFAT pathway, which plays important roles in endothelial inflammation. In addition, we provide evidence suggesting that BMPER may initiate its own signaling pathways via LRP1, which expands our understanding of the roles of BMPER in vascular homeostasis.

How might BMPER play a pro-inflammatory role in LPS-induced acute lung injury? Our gene expression profiling analysis provided us a clue by suggesting that BMPER may regulate NFAT transcriptional activity. We then confirmed that BMPER is not only required but also sufficient for NFAT activation, which plays an essential role in proinflammatory cytokines production in endothelial cells during LPS-induced endotoxemia.[30] This BMPER-induced signaling event involves coordinative actions of multiple pathways. As we propose in the working model (Figure 3.11), BMPER activates ERK pathway in a LRP1-dependent manner, which is required for NFAT activation. Although it remains to be further determined how calcium/calcineurin signaling is activated by BMPER, the studies with calcineurin inhibitor cyclosporine suggest that calcium/calcineurin is also required for BMPER-induced NFAT activation. In addition, we discovered that LRP1β is associated with NF45 in the nucleus at basal condition. Upon BMPER stimulation, they are translocated to cytoplasm in a timely fashion when NFATc1 is translocated to the nucleus. Given that NFATc1 and NF45 are associated with the same promoter regions of their genes, these observations indicate that

NF45 may suppress NFAT transcriptional activity at basal condition. Upon the stimulation, the replacement of NF45 by NFAT transcriptional complex could be allowed in a fast fashion, which may explain the quick transcriptional events for pro-inflammatory cytokines. These timely reactions of endothelial cells, acting as the first line of defense, are essential for fighting against septic shock and the resolution of the acute inflammation.

We, and others, have identified both pro- and anti-BMP activities of BMPER,[13,21,58–65] resulting in some controversy as to whether BMPER is a BMP agonist or antagonist. To reconcile this issue, we have extensively analyzed the biochemical events resulting from BMPER's interaction with BMP4 and identified a concentration-dependent switch of BMPER from pro- to anti-BMP signaling, which is modulated by the relative concentration of BMPER to BMP.[35] Specifically, when BMPER is at molar concentrations lower than BMP4 (sub-stoichiometric), BMP4 activity is enhanced, leading to increased phosphorylation of Smad1/5/8 in mouse endothelial cell. However, when BMPER is at molar concentrations higher than BMP4 (supra-stoichiometric), BMP4-mediated Smad1/5/8 phosphorylation is attenuated. Both the activation and inhibition of BMP4 signaling by BMPER require endocytosis of BMPER/BMP4 complex through a clathrin-dependent endocytosis pathway, suggesting that endocytosis of BMPER/BMP4 complex is involved in BMPER-mediated BMP4 signaling. This provides molecular mechanisms to support a role of BMPER in fine tuning BMP signaling at the single cell level. However, it may not necessarily explain all the pro- and anti- BMP phenotypes in different animal models. In this study, we provide strong evidence suggesting that BMPER, besides acting as an extracellular modulator of BMP, may also initiate its own signaling through LRP1 in endothelial cells. Even though this adds another layer of complexity to BMPER's functional roles, it provides feasible explanations for BMPER's different, sometimes even controversial, loss-of-function phenotypes in different animal models.

LPS-induced NFAT pathway plays a pivotal role in vascular endothelial activation. In endothelial cells, TLR4, and likely CD14 too, are main receptors of LPS. However, it is

unclear whether TLR4 and/or CD14 are required for NFAT activation. In this study, we have discovered that BMPER is required and sufficient for NFAT activation. It will be interesting to determine how BMPER regulates LPS-induced NFAT activation. LRP1 has been reported to transactivate Trk receptors through a Src family kinase-dependent pathway.[66] It is likely that cross-talk may also exist between LRP1 and TLR4, CD14 and/ or their downstream mediators, which coordinately regulate NFAT activation. The detailed protein-protein interactions responsible for this cross-talk will become one of our future research directions.

It is worth noting that the decrease of BMPER expression in the $BMPER^{+/-}$ mouse is not limited to endothelial cells. Since BMPER is a secreted protein, it can act on many different cell types. Additionally, inflammation is a multi-cellular process that involves not only endothelial cells but also other cells such as circulating leukocytes and lung epithelial cells. While our investigation has focused on lung endothelial cells, the role of BMPER in sepsis or other lung inflammatory pathologies may be more complicated than what we observed within this endotoxemia model. Previous studies show that the decreased BMPER expression following bleomycin-induced lung injury impairs epithelial barrier function and epithelial morphology.[67] It is very likely that BMPER haploinsufficiency also regulates functions of epithelial cells, neutrophils or other cell types during LPS-induced acute lung injury, which remains to be further investigated. Nevertheless, given that BMPER is accessible as a secreted protein, our findings shed light that BMPER may become a great therapeutic target during endotoxemia, septic shock, and other pulmonary inflammatory conditions.

3.4 MATERIALS AND METHODS

3.4.1 ANIMALS

$BMPER^{+/-}$ mice, previously created in our lab, and maintained on a C57BL/6 background. $BMPER^{+/-}$ and $BMPER^{+/+}$ were generated from this colony, and male mice aged 10-12 weeks were used. Mice were housed in micro-isolator cages under pathogen-free

conditions and subjected to 12-hour light/dark cycle. The Baylor College of Medicine Institutional Animal Care and Use Committee approved all animal studies, and all experimental procedures were performed according to the National Institutes of Health *Guide for the Care and Use of Laboratory Animals*.

3.4.2 REAGENTS

Recombinant BMPER protein was purchased from R&D Systems (Cat.1956-CV; Minneapolis, MN). Cyclosporin A (CsA) was purchased from Sigma (Cat. C1832; St. Louis, MO) and U0126 was purchased from EMD Millipore (Cat. 19-147; Billerica, MA). The Smad6 construct was purchased from Addgene (Cambridge, MA). The following antibodies were used for immunoblotting: LRP1 purchased from Sigma (Cat. L2170; St. Louis, MO), NF45 antibody purchaced from Santa Cruz Biotechnology (Cat. Sc-271718; Santa Cruz, CA), Lamin B1 and HSP90 purchased from Cell Signaling Technology (cat. 12586, 4877; Danvers, MA), and NFATc1 purchased from BD Pharmingen (Cat. 556602; San Jose, CA).

3.4.3 MODEL OF ENDOTOXEMIA

Lipopolysaccharide (LPS) from *E. coli* serotype O111:B4 was purchased from Calboichem/EMD Millipore (Cat. 437627-5mg; Billerica, MA) for cellularity, total protein and cytokine studies, The LPS was reconstituted in sterile saline (1.0 mg/ml) and mice were given 10 mg/kg intravenously (i.v.) via tail vein. Mice were sacrificed 6 hours after LPS injection and serum or BALF samples were collected.

3.4.4 CAPILLARY LEAKAGE-MILES ASSAY

Evans blue dye (EBD; 1% w/v) was dissolved in PBS and injected into the tail vein of mice 12 hours after LPS injection to assess pulmonary capillary permeability. After 30 minutes, animals were euthanized and their lungs were perfused with 2 ml PBS. The lungs were then excised, placed in a 2.0 ml tube in a 60°C heat block for 48 hours. The lung was then homogenized in 0.03 ml of formamide per 1 mg of dry tissue, and incubated at 60°C for additional 24 hours. The EBD was then extracted by centrifuging lung tissue samples at

5,000 x g for 30 minutes. The supernatants were collected and the absorbance was measured at 620 and 740nm using a Tecan Infinite® 200 Pro microplate reader. The EBD concentration was determined from standard absorbance curves that were measured in parallel. To correct for contaminating heme pigments, the following formula was used: EBD=E620 – (1.426 x E740 + 0.030).

3.4.5 LUNG WET/DRY RATIO

For determination of lung wet/dry ratios, the whole lung was excised, cleaned and weighed. The lung was then placed in a 2 ml tube and incubated at 60°C (dry heat) with the tube lid open for 48 hours. Then weighed a second time and the wet-to-dry weight calculated.

3.4.6 LUNG HISTOLOGY

Harvested lungs were fixed in 10% formalin. Tissues were embedded in paraffin. Five micrometer-thick sections were stained with H&E and analyzed by light microscopy. Lung injury was graded from 1 (normal) to 4 (severe) in four categories: interstitial inflammation, neutrophil infiltration, congestion, and edema according to previous reports.[68,69] The injury score was calculated by adding the individual scores for each category. Scoring was performed blindly. Lung tissues were also prepared for frozen sectioning. The frozen sections were used for immunofluorescent imaging and NF45 translocalization studies.

3.4.7 BAL FLUID COLLECTION

Bronchoalveolar lavage (BAL) fluid (BALF) was obtained by flushing 3x 0.8 ml aliquots of saline into the lung via a tracheal cannula. The pooled BALF was centrifuged at 500 x g at 4°C for 5 minutes. Cell pellets were then resuspended in 500 µl PBS and the total cell number was counted using a hemocytometer. The supernatant of BALF was stored at -80°C for subsequent analysis of protein content and cytokine ELISAs.

3.4.8 SERUM COLLECTION

Blood was collected from the submandibular vein 6 hours after LPS injection. Approximately 400-600□l whole blood was captured in amber serum separator BD Microtainer® tubes. Tubes were inverted 5 times, incubated at room temperature 30 minutes, centrifuged 10,000xg 5 minutes, serum (top) layer transferred to labeled 1.5ml tube and stored at -80°C.

3.4.9 BALF PROTEIN QUANTITATION

After centrifugation of BALF samples, total protein concentration was determined using the Bio-Rad Protein Assay per the manufacturer's instructions (Cat. 500-0006; Hercules, CA). Qiying Fan, Ph.D, kindly performed this assay.

3.4.10 CYTOKINE MEASUREMENTS

Serum and BALF levels of TNF-a, IL-6 and IFN-g were measured using ELISA kits (R&D Systems, Minneapolis, MN) according to the manufacturer instructions.

3.4.11 CELL CULTURE AND TRANSIENT TRANSFECTIONS

Mouse primary lung microvascular endothelial cells (MLECs), purchased from Cell Biologics (Chicago, IL), were cultured in MCDB131 basal medium supplemented with 5% FBS, VEGF, ECGS, Heparin, EGF, hydrocortisone, L-glutamine and antibiotic solution. Cells ranging from passage 6-10 were used for experiments. Approximately 70% confluent cells in 6-well plates were transfected for 3 hours with 1 μg of plasmids using 4 μl of Lipofectamine LTX and 4 μl of Plus reagent (Life Technologies) following our previous protocol.[43] Two days later, cells were treated with indicated reagents for further assays. For stably expressed LRP1 in 293 cells, 90-100% confluent 293 cells in 10-cm dishes were transfected 24 hours after plating with 2 μg of Flag-tagged LRP1β plasmid using 20 μl of Lipofectamine 2000 (Life Technologies) and then transfected cells were selected by using Geneticin (G418; Life Technologies).

3.4.12 LUCIFERASE ASSAY

MLECs were transfected with NFAT-responsive or NFκB firefly luciferase and constitutively expressing renilla plasmids (Cignal™ Reporter Assay kits from Qiagen, Valencia, CA). One day later, cells were treated with BMPER or LPS as indicated. Cells were lysed 24 hours later and analyzed with the Dual-Luciferase® Reporter Assay System from Promega (Madison, WI) according to the manufacturer's instructions using a Tecan Infinite® 200 Pro microplate reader.

3.4.13 SUBCELLULAR FRACTIONATION ASSAY

Subcellular fractions (cytosolic and nuclear) were obtained following previous protocol[70] with a slight modification. MLECs were lysed using hypotonic buffer, and the supernatant (cytosolic) and pellet (nuclear fraction) were separated by centrifugation at 15,000 x g for 5 minutes. Purity and consistency of fractions were confirmed using antibodies against markers for different subcellular compartments: anti-HSP90 (cytosolic marker) and anti-Lamin B1 (nuclear marker).

3.4.14 siRNA DESIGN AND TRANSIENT TRANSFECTION

The stealth siRNA duplexes were obtained from Life Technologies. The siRNA against mouse LRP1 is a duplex of 5'-CCAAGGUGUGAGGUGAACAAGUGUA -3'. The siRNAs of mouse NFATc1 (Cat. No. MSS275980), NF45 (Cat. No. MSS228688) and control siRNA (stealth RNAi negative control duplex; Cat. No. 12935-300) were purchased from Life Technologies. The siRNAs were transfected into MLECs according to our previous published protocol.[43] Briefly, for each sample, $2x10^5$ MLECs were transfected with 100 pmol siRNA. The experiments with siRNA transfected MLECs were performed two days later.

3.4.15 REAL-TIME PCR

Total RNAs were reverse transcribed into cDNAs with iScriptTM cDNA synthesis kit (Bio- Rad, Hercules, CA, USA). The specific pairs of primers used for the real-time PCR are

the following: NFATc1 (forward primer: 5'- tccaaagtcattttcgtgga-3' and reverse primer: 5'- ctttgcttccatctcccaga 3'), GAPDH (forward primer: 5'- tgtccgtcgtggatctgac-3' and reverse primer: 5'-cctgcttcaccaccttcttg- 3'); designed by Universal ProbeLibrary Assay Design Center tool (Roche, Indianapolis, IN). The real-time PCR was performed with FastStart Universal Probe Master mix and specific primers and probes for each gene (Universal ProbeLibrary Single Probes #50 for NFATc1, and #80 for GAPDH) in Roche Lightcycler 480 PCR machine. The reaction mixtures were incubated at 95°C for 10 min followed by 55 cycles at 95°C for 10 sec and 60°C for 30 sec. GAPDH was used as the housekeeping gene.

3.4.16 Immunoblotting and Immunoprecipitation

Cells were harvested in lysis buffer (1% Triton X-100, 50 mmol/L Tris (pH 7.4), 150 mmol/L NaCl, 1 mmol/L Na3VO4 and 0.1% protease inhibitor mixture; Sigma) and clarified by centrifugation at 15,000 x g. Proteins were separated by SDS-PAGE and transferred onto 0.45 mm PVDF membranes. Immunoprecipitation experiments were carried out on cell lysates of HEK293 cells or MLECs as indicated. Cell lysates were incubated with flag (Sigma) or protein A/G plus-agarose beads (Santa Cruz Biotechnology) overnight at 4°C with gentle rotation. Immune complexes were then separated by SDS-PAGE and analyzed by Western blot.

3.4.17 Immunofluorescence and Co-localization Analysis

Immunofluorescence with cultured MLECs was performed following our previously published protocol.[43] Cells were cultured on 2% gelatin coated coverslips and fixed in 3.7% paraformaldehyde for 10 min at room temperature. After 3 washes with PBS, cells were sequentially treated with 0.2% Triton X-100 for 5 min (to permeabilize), then 5% boiled serum for 1 hour (for blocking), then with the primary antibody overnight in the blocking solution. After 3 washes, cells were incubated in the dark with secondary antibody conjugated with Alexa Fluor® 568 (Life Technologies) in blocking solution for 90 min at 37°C. After 3 washes in PBS, the slides were mounted and fluorescent signals were imaged

via confocal laser scanning microscopy (Zeiss Pascal, Zeiss, Germany). The relative intensity of LRP1β and NF45 in whole vessels, nuclear and cytoplasmic fractions of each cell was quantified with Image J.

3.4.18 Statistical Analysis

Data are shown as the mean ± SEM for 3 to 4 separate experiments. Differences were analyzed with Student's t-test or ANOVA and followed by a post hoc test with a correction when needed. Values of $P \leq 0.05$ were considered statistically significant.

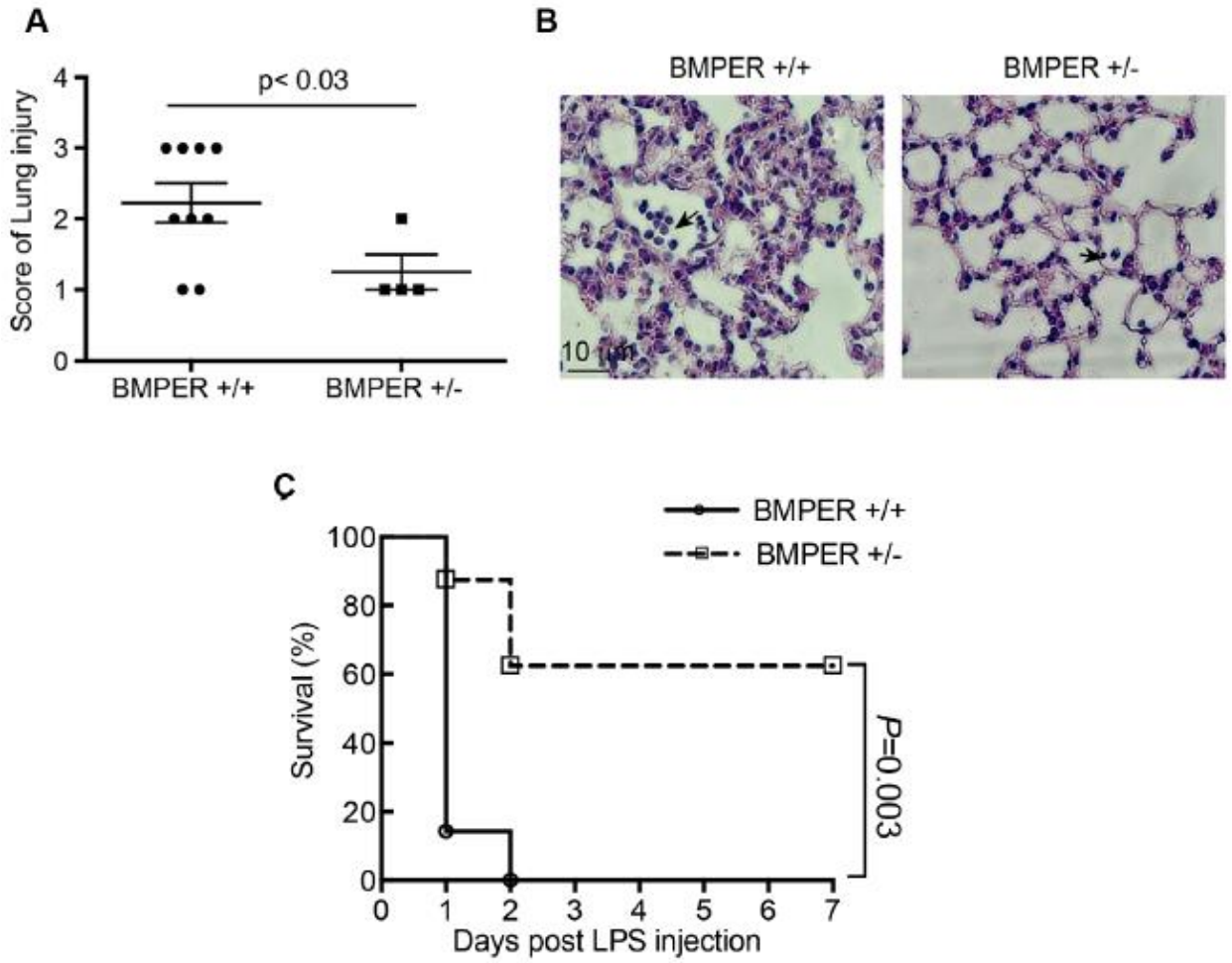

Figure 3-1. BMPER haploinsufficiency attenuates LPS-induced lung injury and promotes survival.

A-B, Lung injury, as determined by injury scoring and histological analysis, is less severe in BMPER$^{+/-}$ mice versus BMPER$^{+/+}$ mice. BMPER$^{+/-}$ or BMPER$^{+/+}$ mice were injected i.v. with a sub-lethal dose (10 mg/kg) of LPS and sacrificed 16 hours later. **A,** Lung tissues were screened for lung injury score. n=9 (BMPER$^{+/+}$) and n=4 (BMPER$^{+/-}$). **B**, Representative photomicrographs of lung tissue stained with hematoxylin and eosin after LPS injection. LPS stimulated infiltration of inflammatory cells into the lung interstitum and alveolar space, alveolar wall thickening and intra-alveolar proteinacious exudation. **C**, Survival curves for BMPER$^{+/-}$ and BMPER$^{+/+}$ mice injected i.v. with a lethal dose of LPS (15 mg/kg). P=0.003; n=7~8. Analysis, Student's unpaired t-test (**A**) log-rank test (**C**).

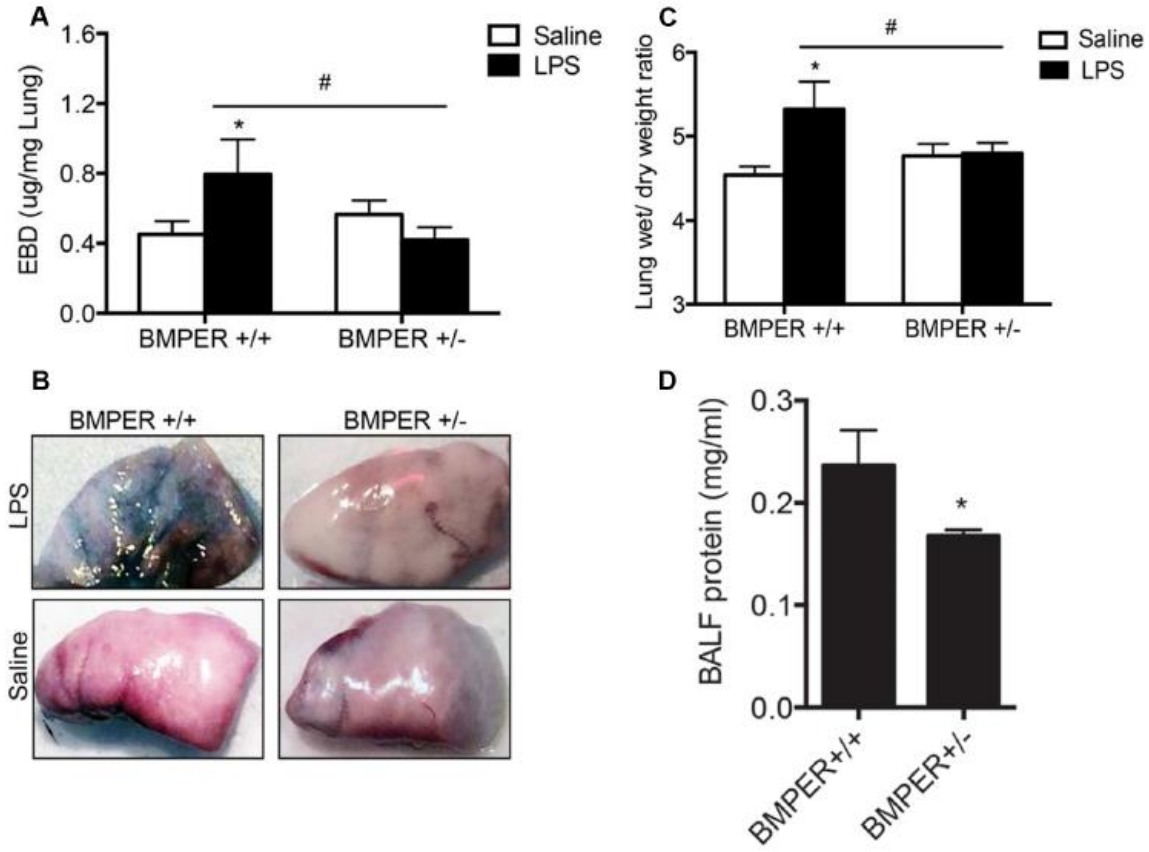

Figure 3-2. BMPER haploinsufficiency attenuates LPS-induced pulmonary vascular permeability.

All measures of LPS-induced capillary leakage (**A**,**B**), edema (**C**) and BALF protein content (**D**)are reduced in BMPER$^{+/-}$ versus BMPER$^{+/+}$ mice. BMPER$^{+/-}$ or BMPER$^{+/+}$ mice were injected with a sub-lethal dose (10 mg/kg i.v.) of LPS and 16 hours later given a bolus of Evans Blue dye (EBD; 1% w/v). Mice were sacrificed 30 minutes later. Representative lung tissues with extravated EBD were photographed and shown in (**B**). *P<0.05, compared with mice injected with saline (**A**,**C**) or BMPER$^{+/+}$ mice (**D**); #P<0.05 compared with BMPER$^{+/+}$ mice (**A**,**C**).). Analysis, two-way ANOVA followed by Fisher's LSD multiple comparison test (**A**,**C**) and unpaired Student's t-test (**D**).

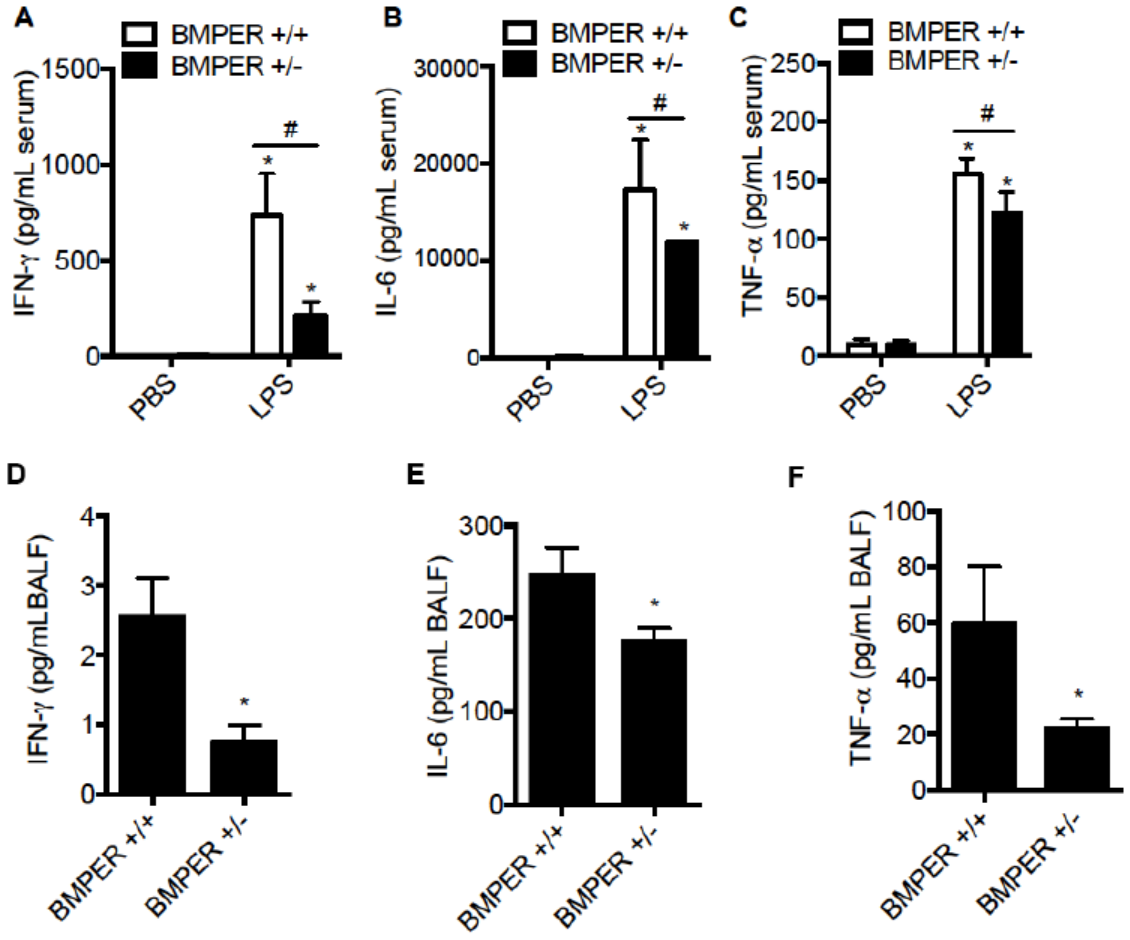

Figure 3-3. BMPER haploinsufficiency reduces proinflammatory cytokines both systemically and in BALF after LPS challenge.
BMPER$^{+/+}$ and BMPER$^{+/-}$ mice were treated with LPS (10 mg/kg i.v.) or PBS (**A-C**), and after 6 hours indicated cytokine concentrations were measures in sera and BALF extracts (**A-F**). *P<0.05, compared with same mice injected with PBS (**A-C**) or BMPER$^{+/+}$ mice (**D-F**); #P<0.05, compared with BMPER+/+ mice (**A-C**). Analysis, two-way ANOVA followed by Fisher's LSD multiple comparison test (**A-C**) and unpaired Student's t-test (**D-F**).

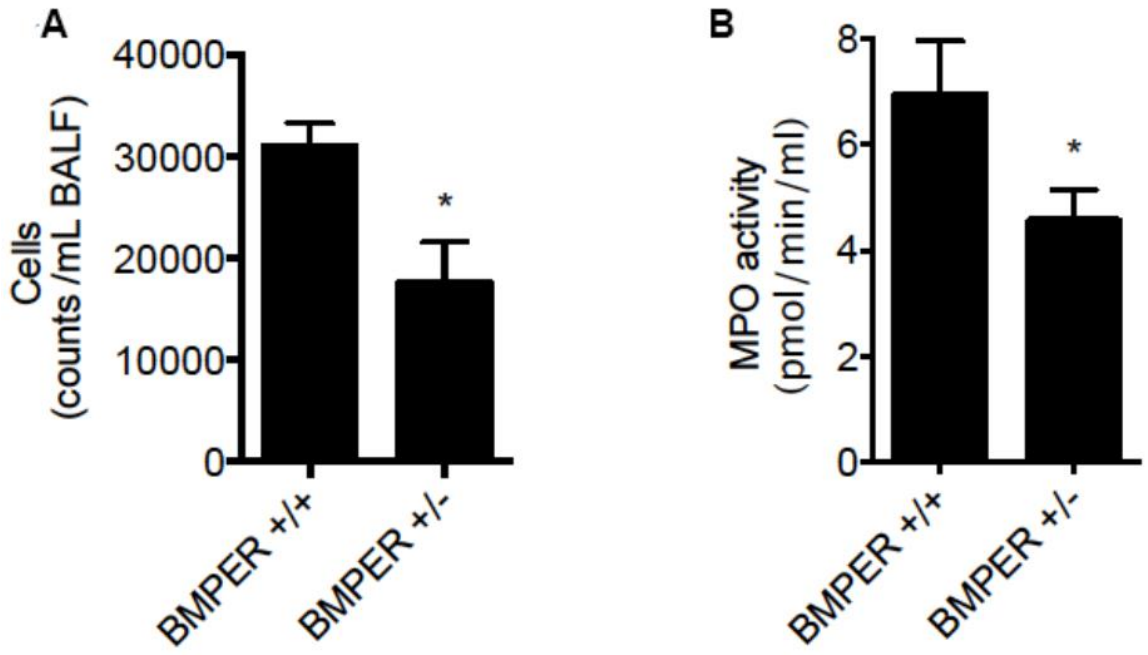

Figure 3-4. LPS-induced migration of leukocytes is reduced in BMPER+/- mice.
BMPER+/- mice had lower cell numbers (**A**) and myeloperoxidase activity (**B**) in BALF extracts 6 hours after LPS treatment (10 mg/kg i.v.). *P<0.05, compared with BMPER$^{+/+}$ mice; n=4~9. Analysis, unpaired Student's t-test.

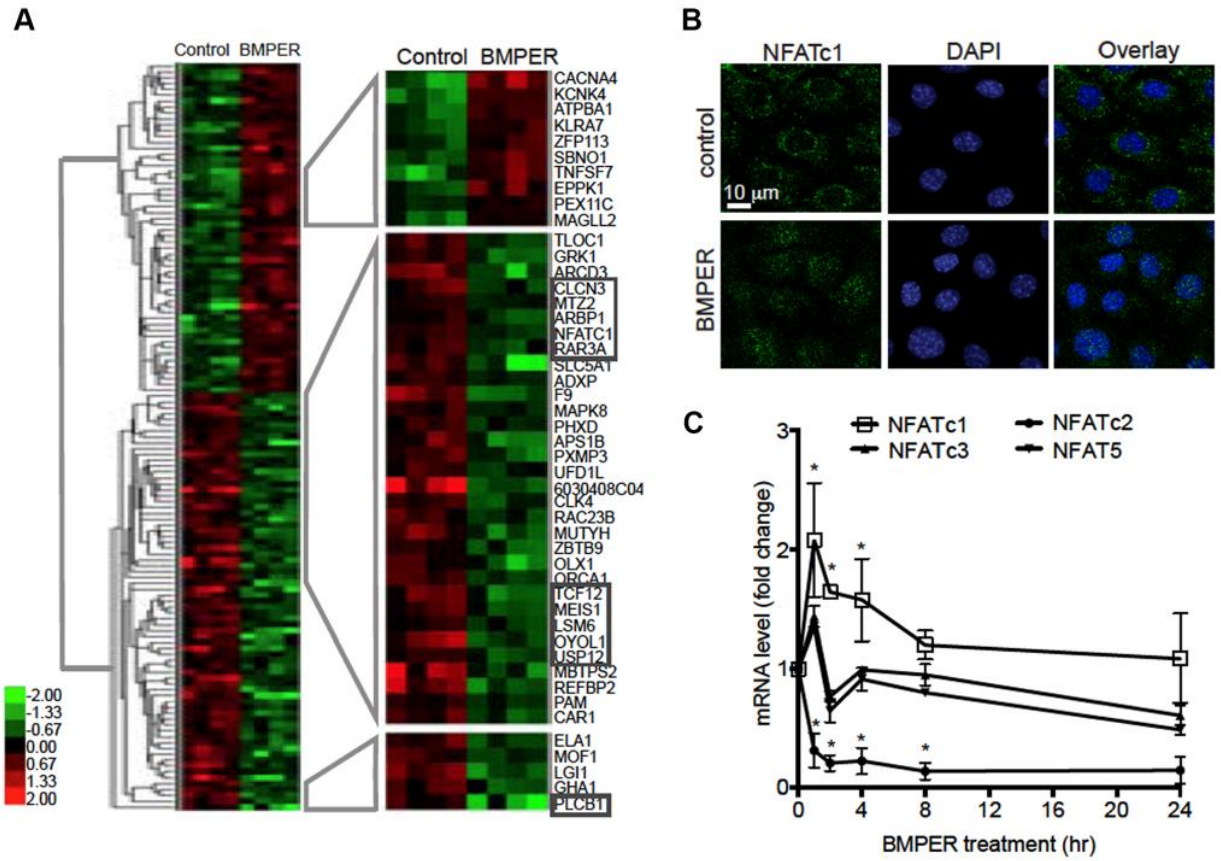

Figure 3-5. BMPER induces NFAT-dependent target genes, including NFATc1.
A, Hierarchical clustering was performed with microarray data of mouse cardiac-derived endothelial cells treated with BMPER at 10nM or control for 4 hours. Fold change relative to common reference is indicated by red and green intensity. Specific clusters of genes containing NFAT-responsive elements in their promoters are boxed. B, BMPER increases NFAT translocation from cytoplasm into nucleus in endothelial cells. Mouse cardiac-derived endothelial cells were treated with 10 nM BMPER for 30 minutes. The representative images were taken with confocal microscopy. **C**, BMPER induced NFAT transcriptional factors in endothelial cells. MLECs were treated with 10 nM BMPER for indicated time periods. NFATc4 is not detectable. NFATc1 is the most induced isoform of NFAT transcriptional factors. * $P<0.05$; n=3. Analysis, two-way ANOVA followed by Fisher's LSD multiple comparison test.

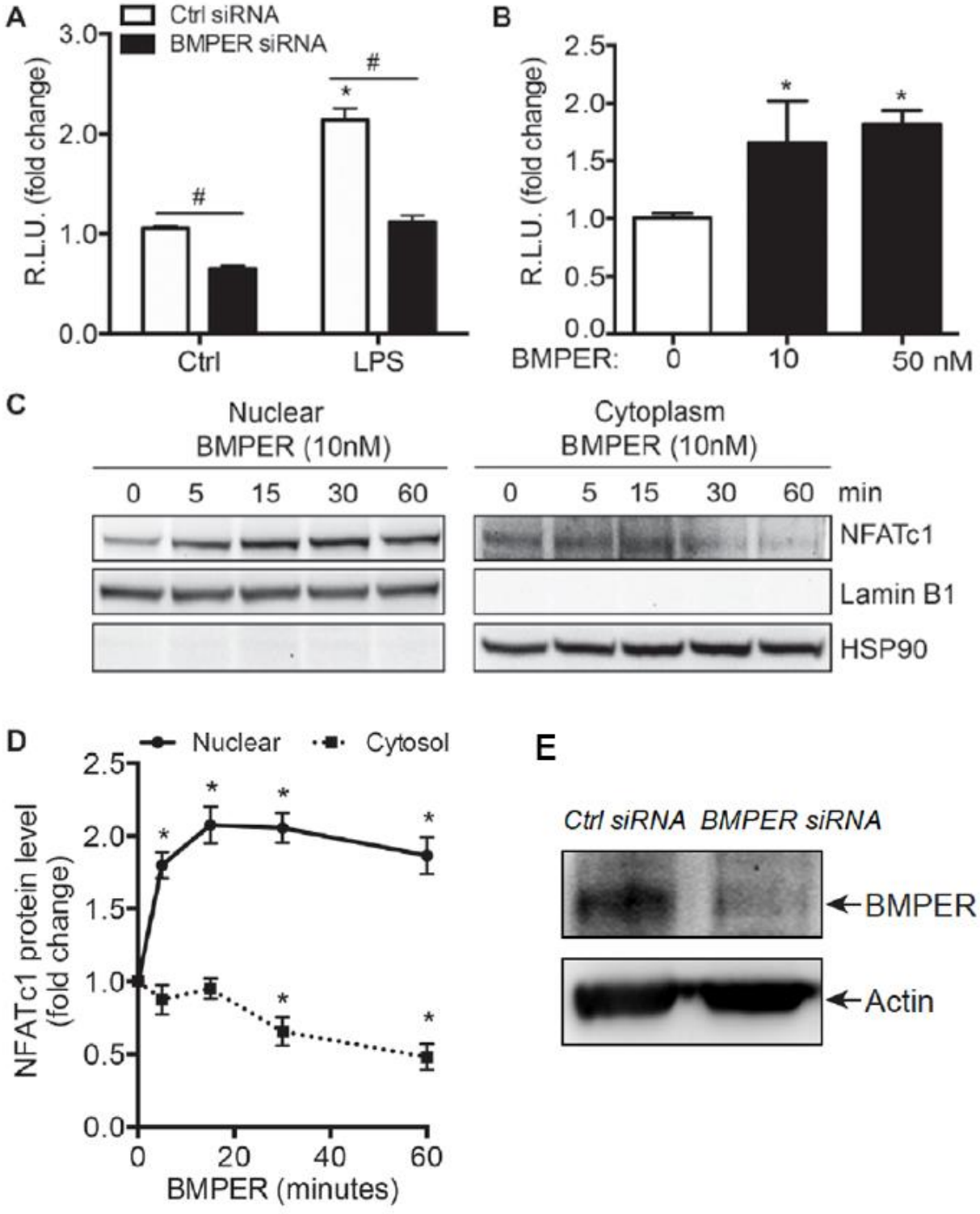

Figure 3-6. BMPER is required and sufficient to activate NFATc1.
A, BMPER knockdown blocks NFAT activation in response to LPS (10 μg/ml). MLECs were transfected with a mixture of NFAT-responsive firefly luciferase and renilla constructs, and BMPER or control siRNA. One day later, cells were treated with LPS and the luciferase activity was measured

after another day's incubation. (**B)**, BMPER increases transcriptional activity of NFAT in MLECs. MLECs were transfected with a mixture of NFAT-responsive firefly luciferase and renilla constructs. After 24 hours, cells were treated with BMPER or control for another 24 hours and the luciferase activity was measured. (**C-D)**, BMPER increases nuclear translocation of NFATc1. MLECs were treated with 10 nM BMPER for indicated time periods. Nuclear and cytoplasmic enriched fractions of cell lysates were used to determine the translocation of NFATc1. Lamin B1 (nuclear marker) and HSP90 (cytosol marker) immunoblotting were used to verify the purity of the fractions. NFATc1 protein levels in nuclear and cytosol fractions were quantified and shown in (**D**). * $P<0.05$, compared to cells without LPS (**A**) or BMPER (**B**,**D**) treatment; # $P<0.05$; n=3~6. Analysis was two-way ANOVA followed by Fisher's LSD multiple comparison test (**A**) and one-way ANOVA (**B**, **D**). (*******Data for figure (**A)** provided by Hua Mao, Ph.D.)

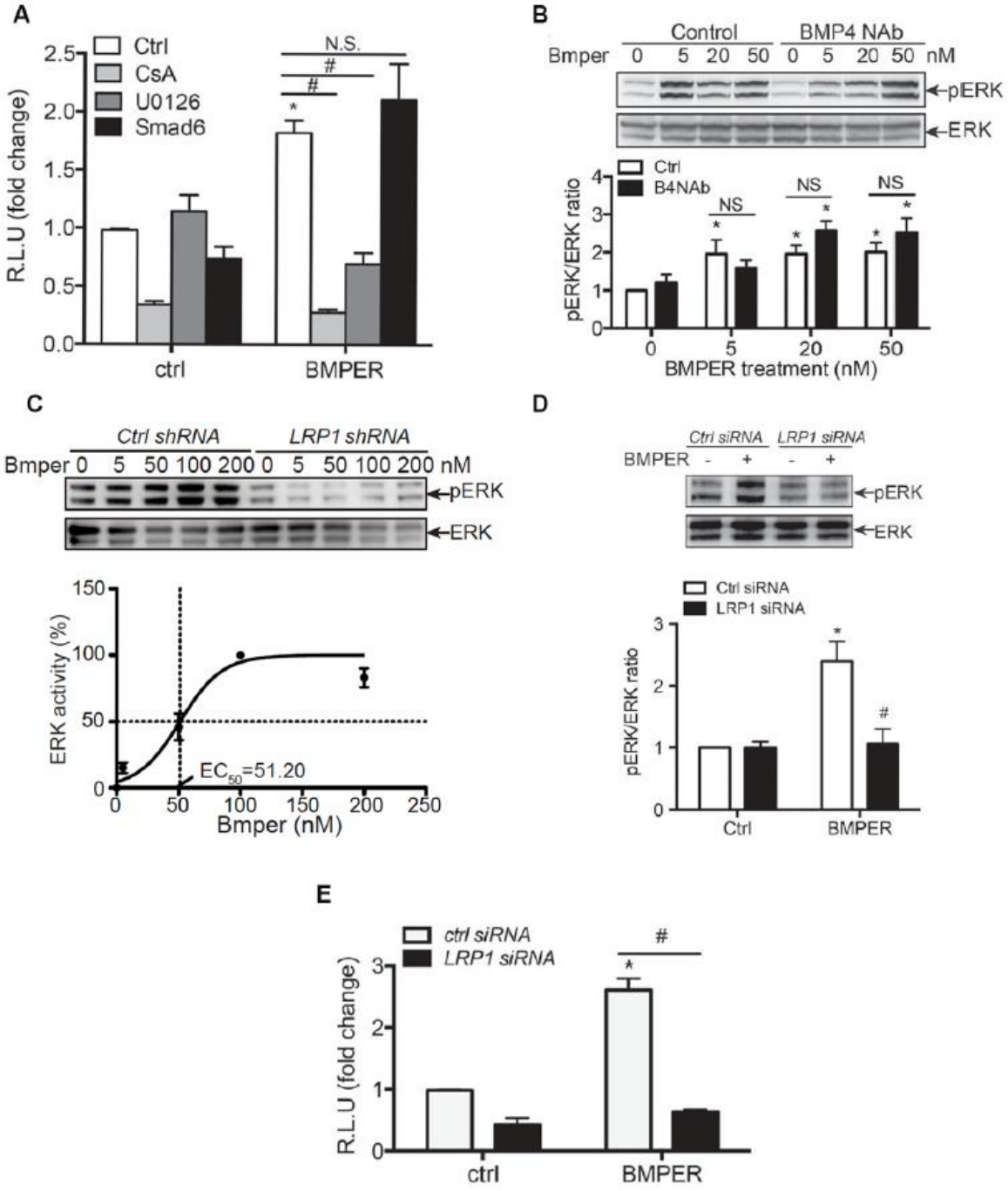
A
Ctrl
CsA
U0126
Smad6
R.L.U (fold change)
N.S.
ctrl
BMPER
B
Control
BMP4 NAb
Bmper 0 5 20 50 0 5 20 50 nM
pERK
ERK
Ctrl
B4NAb
pERK/ERK ratio
NS
BMPER treatment (nM)
C
Ctrl shRNA
LRP1 shRNA
Bmper 0 5 50 100 200 0 5 50 100 200 nM
pERK
ERK
ERK activity (%)
EC50=51.20
Bmper (nM)
D
Ctrl siRNA
LRP1 siRNA
BMPER - + - +
pERK
ERK
pERK/ERK ratio
Ctrl
BMPER
E
ctrl siRNA
LRP1 siRNA
R.L.U (fold change)
ctrl
BMPER

Figure 3-7. LRP1 is required for BMPER induced NFAT activation.
A, Inhibitors of calcineurin and ERK pathways block NFAT activation upon BMPER treatment. MLECs were transfected with constructs of NFAT-responsive luciferase, renilla and inhibitory Smad-Smad6. After 24 hours, cells were pre-treated with cyclosporine A (CsA), U0126 for half an hour and then treated with BMPER or control. Luciferase activity was measured after another day's incubation. **B**, BMPER-induced ERK activation is not inhibited by BMP4 neutralizing antibody in MECs. Mouse cardiac-derived endothelial cells were treated with BMPER at indicated doses for 30 minutes. BMP4 neutralizing antibody (Nab; 40 ng/ml) was used to pretreat cells to block BMP4 activity. **C,** BMPER increases LRP1-dependent ERK activation. MECs stably transfected with LRP1 shRNA or control shRNA were treated with BMPER at different doses for 30 minutes, and then harvested for Western blotting. ERK activity was calculated by measuring the intensity of phosphor-ERK and total ERK blots, and the value of ERK activity for samples with BMPER treatment at 50 nM was considered 100% for the calculation of EC50 value. **D**, BMPER increases LRP1-dependent ERK activation. MLECs transiently transfected with LRP1 siRNA were treated with BMPER at 10 nM for 30 minutes, and then harvested for Western blotting. ERK activity was calculated by measuring the intensity of phosphor-ERK and total ERK blots. **E**, LRP1 is required for NFAT activation induced by BMPER. MLECs were transfected with LRP1 or control siRNA, and NFATresponsive luciferase and renilla constructs. After 24 hours, cells were treated with BMPER or control. Luciferase activity was measured after another day's incubation. $P<0.05$, compared to control cells without BMPER or other indicated treatments; # $P<0.05$, compared as indicated (**A**, **B**, **D**) or to control siRNA transfected cells upon same treatments; n=3~4. NS, not significant. Analysis, two-way ANOVA followed by Fisher's LSD multiple comparison test. (***Figures D and E,** data provided by Hua Mao, Ph.D.)

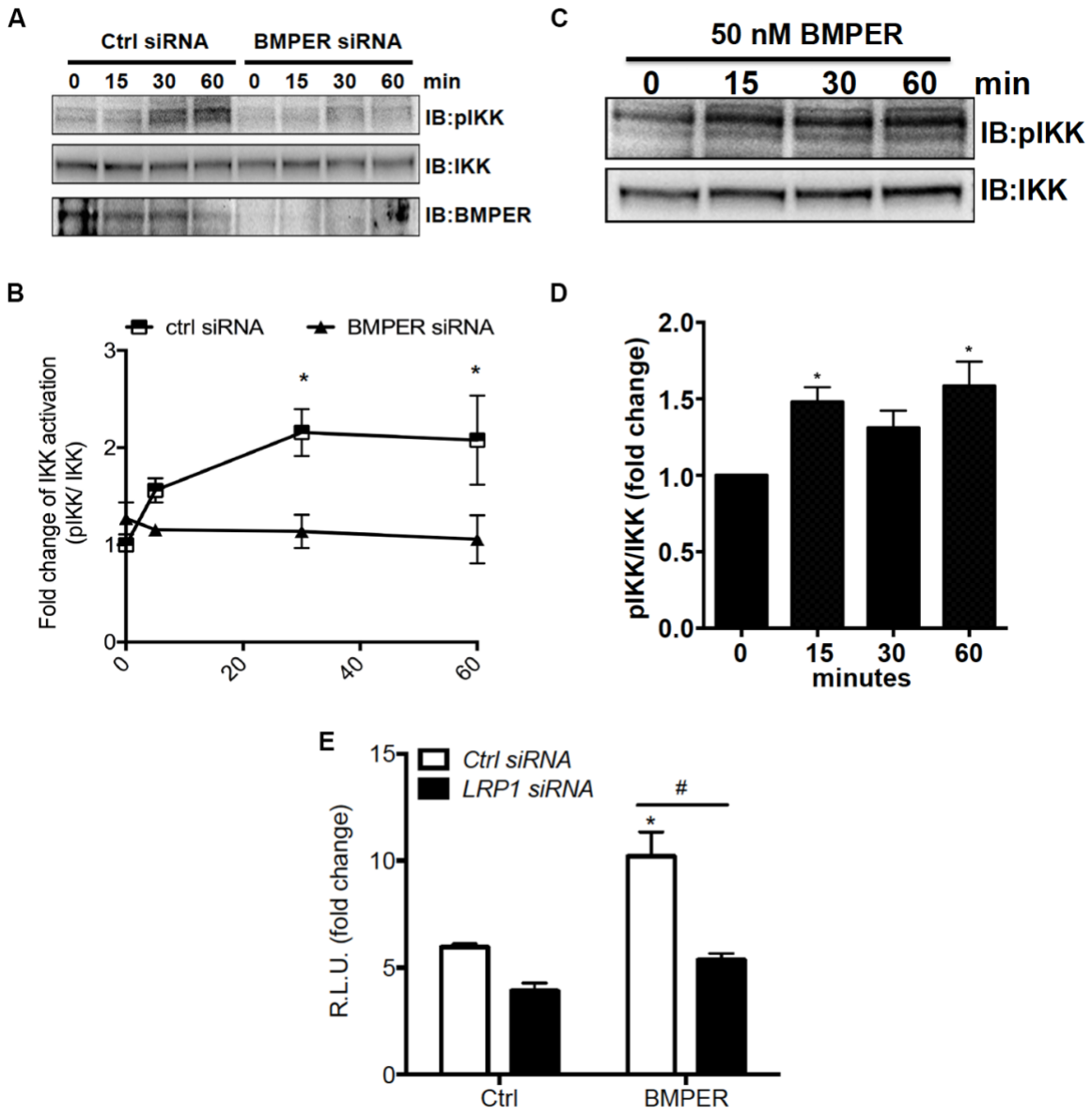

Figure 3-8. BMPER/LRP1 induces NFκB activation.
A, BMPER knockdown blocks IKK phosphorylation in MLECs in response to LPS (10ug/ml) over time. **B,** quantitation of the data in **A** showing the activation of IKK, as measured by the ratio of the phosphorylated IKK to the total IKK. **C**, BMPER alone induces IKK phosphorylation in MLECs. Cells were treated with 10nM BMPER over a period of time and Western blot studies were performed with cell lysates. **D,** is the quantitative data of **C** showing the activation of IKK, as measured by the ratio of the phosphorylated IKK to the total IKK. $p<0.05$, compared to control. n=3. Analysis was one-way ANOVA (**B**,**D**), unpaired Student's t-test (**F**) and two-way ANOVA followed by Fisher's LSD multiple comparison test (**G**). (***Figure 3.8G, Dr. Hua Mao)

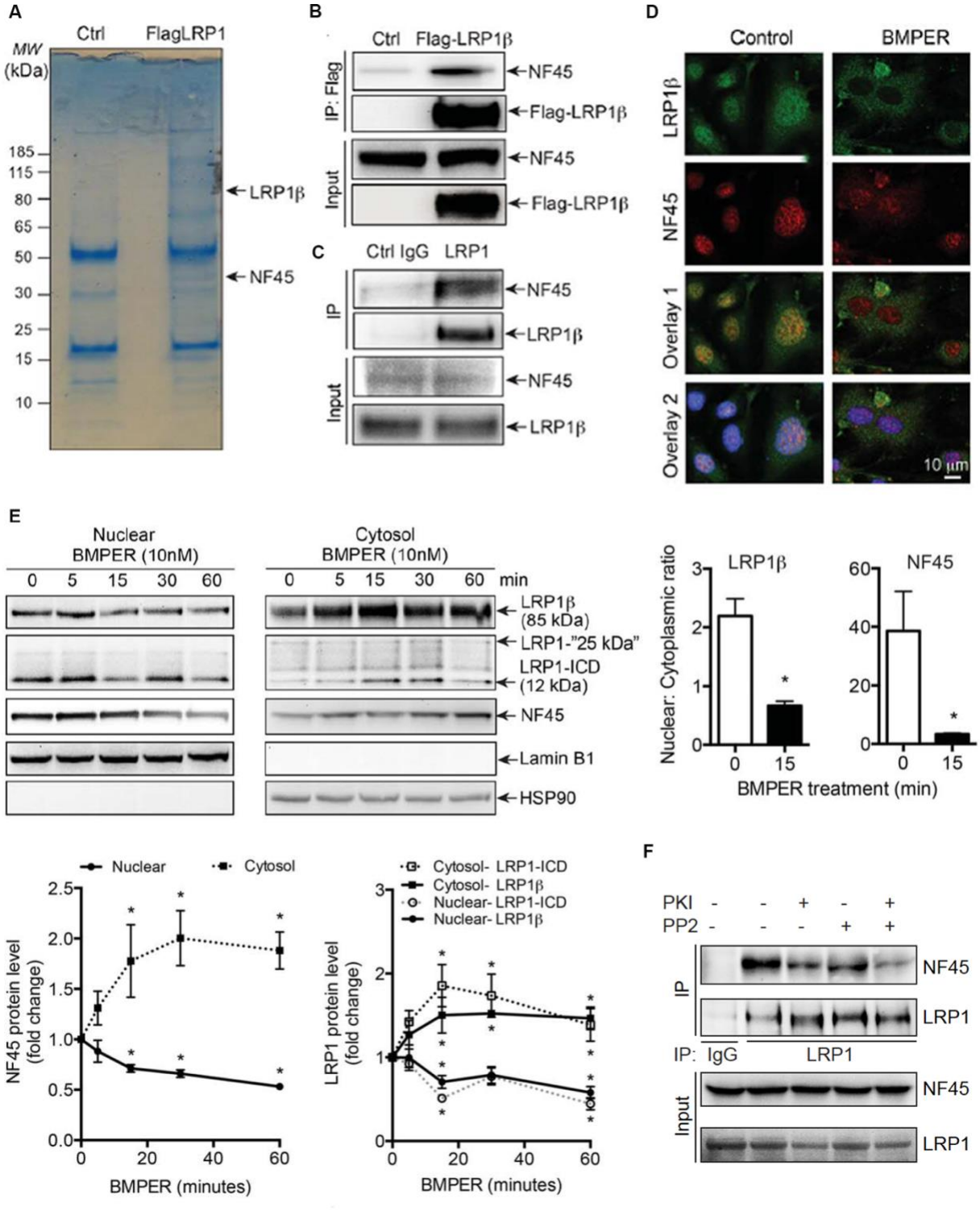

Figure 3-9. NF45 is associated with LRP1β and involved in NFAT activation.
A, NF45 is a candidate protein associating with LRP1. Lysates of HEK 293 cells with stably transfected Flag-tagged LRP1 β chain (Flag-LRP1β) were immunoprecipitated with an anti-Flag antibody and stained with Coomassie blue. Positive bands are subjected to mass spectrometry

analysis to identify interacting proteins. NF45 is one of these candidate proteins that are likely associated with LRP1. **B**, Flag-tagged LRP1β is associated with NF45 in HEK293 cells. Lysates of HEK 293 cells with stably expressing Flag-LRP1β were immunoprecipitated with an anti-flag resin and blotted with an anti- NF45 antibody. **C**, LRP1β is associated with NF45 in MLECs. Lysates of MLECs were immunoprecipitated with anti-LRP1β antibody or control IgG, and analyzed by Western blotting with an anti-NF45 antibody. **D-E**, LRP1β and NF45 are translocated from nucleus to cytoplasm upon BMPER treatment. MLECs were treated with BMPER at 10 nM for 15 minutes. After fixation, cells were stained with LRP1 (C-terminal) antibody (green), NF45 antibody (red) and DAPI (blue) for nucleus and representative pictures were shown in **D**. LRP1 (C-terminal) antibody recognizes both LRP1β and its processed fragments at 25 kDa and 12 kDa intracellular domain. The relative intensity of LRP1β and its processed fragments, and NF45 in nuclear and cytoplasmic fractions was quantified and the ratios of nuclear to cytoplasmic signals were presented in **D**. * $P<0.05$, compared to control cells; n=8~12. In addition, MLECs were treated with BMPER and fractionation assays was performed. Band intensity of LRP1β, its intracellular domain at 12 kDa (LRP1-ICD) and NF45 was calculated and normalized to the sample without BMPER treatment. The graph in **E** shows a decrease in nuclear NF45, LRP1β and LRP1-ICD protein levels but an increase in cytosolic NF45, LRP1β and LRP1-ICD. The protein level of the LRP1β processed form at 25 kDa was not changed in the cytosol in response to BMPER treatment. * $P<0.05$, compared to cells without BMPER treatment; n=3. **F**, NF45 knockdown promotes NFAT activity. MLECs were transfected with a mixture of NFAT-responsive firefly luciferase and renilla constructs, and NF45 or control siRNA. One day later, cells were treated with BMPER at 10 nM and the luciferase activity was measured after another day's incubation. **G**, The interaction of LRP1β with NF45 is phosphorylation-dependent. MLECs were treated with PKI (10μM), PP2 (1 μM) or both for one hour. Cell lysates were immunoprecipitated with anti-LRP1 antibody or IgG as control and then immunoblotted for NF45. *$P<0.05$, compared to cells without BMPER treatment; #$P<0.05$; n=3. Analysis was Student's t-test (**D**), one-way ANOVA (**E**) and two-way ANOVA followed by Fisher's LSD multiple comparison test (**F**). (***Figures B, C, F** and **G;** data provided by Hua Mao, Ph.D.)

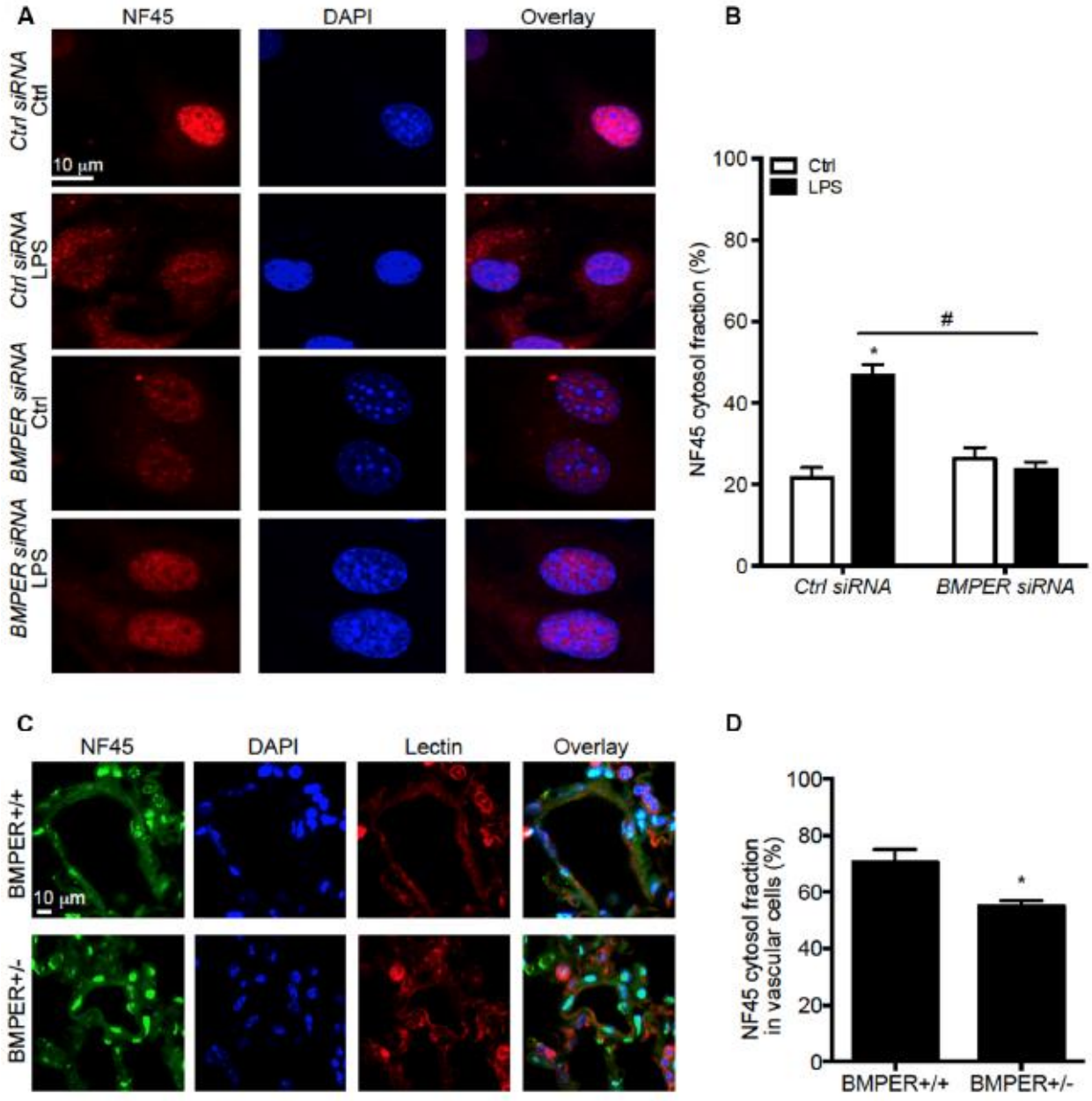

Figure 3-10. NF45 is regulated by BMPER/LRP1 signaling.

A-B**,** BMPER knockdown blocks NF45 nuclear export upon LPS treatment. MLECs were transfected with BMPER or control siRNA. Two days later, cells were treated with 10 μg/ml LPS for 15 minutes. Cells were stained with NF45 antibody (red) and DAPI (blue) for nucleus and representative pictures were shown in A. The relative intensity of NF45 in nuclear and cytoplasmic fractions was quantified. Fractions of cytoplasmic signals were presented in B. * $P<0.05$, compared to cells without LPS treatment; # $P<0.05$; n=14. **C**-**D**, BMPER haploinsufficiency decreases cytosol localization of NF45 in vascular cells of lung sections. $BMPER^{+/-}$ or $BMPER^{+/+}$ control mice were injected with 10 μg/kg LPS and their lungs were harvested for histology. Cells were stained with NF45 antibody (green), lectin (red) for vascular cells and DAPI (blue) for nucleus. Representative pictures were shown in C. The intensity of NF45 positive signals in each vessel and all the vascular cell nuclei was measured. Fractions of cytosol signals were calculated and normalized by the number of vascular cells in each vessel. The quantitative data is presented in D. * $P<0.05$; n= 3 vessels per mouse section and 3 mice per group. Analysis was two-way ANOVA followed by Fisher's LSD

multiple comparison test (B) and unpaired Student's t-test (D). (***Data for figures A-D provided by Dr. Hua Mao)

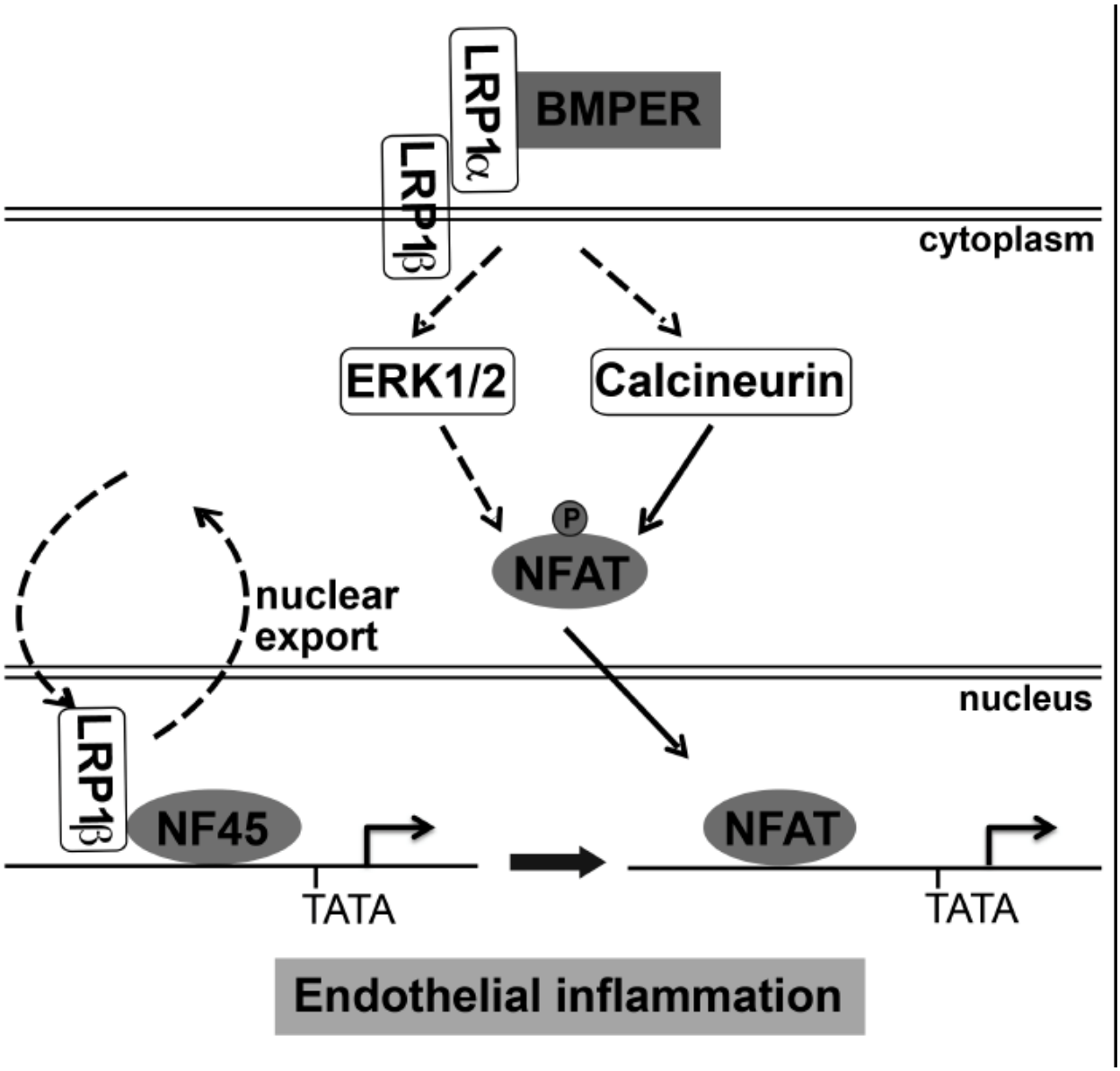

Figure 3-11. Schematic illustration showing how BMPER regulates NFATc1 activation via coordination of LRP1, ERK, calcineurin and NF45.

\

CHAPTER 4:SUMMARY

The experiments described herein attempt to characterized the role of BMPER in the vascular response to stress and injury by uncovering the BMPER-dependent signaling events and their role in pathophysiologic inflammatory conditions such as atherosclerosis and sepsis. Data generated here reveal that 1) BMPER is a novel player in atherosclerosis and fluid-shear stress mediated chronic inflammatory responses in endothelial cells, 2) mechanistically, BMPER exerts protective effects by inhibiting BMP activity, 3) inhibition of BMPER signaling limits endotoxemia-induced acute inflammatory responses in the pulmonary endothelium and 4) BMPER regulates acute inflammatory responses through the NFATc1 pathway independent of BMP signaling. Earlier studies have identified essential roles for BMPER in endothelial cell differentiation, migration and angiogenesis through BMPER's regulation of BMP signaling.[1–6] Our examination of BMPER here identifies a novel role for BMPER in mediating both acute and chronic vascular inflammation. Yet the story is not straightforward. Since its discovery, BMPER has been frought with controversy as to whether it promotes or inhibits BMP signaling, and at first glance it may seem there results here only further complicate our knowledge of BMPER's function in the vasculature.

The first study presented here clearly shows BMPER to have protective anti-inflammatory effects during chronic inflammation and atherosclerosis, a chronic inflammatory disease. ApoE-/- mice with reduced BMPER expression have smaller

atherosclerotic lesions with less calcification. Also, when subjected to oscillatory shear stress, BMPER reduces the expression of the inflammatory adhesion molecules ICAM1 and VCAM1 in endothelial cells. The second study identifies BMPER as a pro-inflammatory mediator in the vasculature during acute inflammation and endotoxemia. Previous mouse models of thioglycollate-induced peritonitis and high fat-induced atherosclerosis[7–9] suggest an anti-inflammatory role for BMPER through mediating BMP-signaling. We identify, for the first time, a BMP-independent role for BMPER to expand our understanding of how BMPER regulates vascular homeostasis. We show that in an acute inflammatory mouse model of endotoxemia that BMPER promotes pulmonary endothelial permeability and edema, while reduced BMPER expression enhances survival. We show biochemically that BMPER activates NFAT inflammatory signaling through a novel BMP-independent but LRP1-dependent pathway. As compelling as our results may be, they warrant further investigation. Both atherosclerosis and sepsis are complex, multifactorial pathologic conditions that result from the dysfunction of many cell types, tissues, genetic and environmental factors. Nevertheless, given that BMPER is accessible as a secreted protein, our findings shed light that BMPER may become a therapeutic choice during atherosclerosis, endotoxemia, sepsis shock, and other inflammatory conditions.

REFERENCES

1. Aird, W. C. Endothelium as an organ system. *Crit. Care Med.* **32,** S271-279 (2004).

2. Aird, W. C. Phenotypic heterogeneity of the endothelium: I. Structure, function, and mechanisms. *Circ. Res.* **100,** 158–173 (2007).

3. Rajendran, P. *et al.* The vascular endothelium and human diseases. *Int. J. Biol. Sci.* **9,** 1057–1069 (2013).

4. Cines, D. B. *et al.* Endothelial Cells in Physiology and in the Pathophysiology of Vascular Disorders. *Blood* **91,** 3527–3561 (1998).

5. Endemann, D. H. & Schiffrin, E. L. Endothelial Dysfunction. *JASN* **15,** 1983–1992 (2004).

6. Mai, J., Virtue, A., Shen, J., Wang, H. & Yang, X.-F. An evolving new paradigm: endothelial cells--conditional innate immune cells. *J Hematol Oncol* **6,** 61 (2013).

7. Vita, J. A. Endothelial Function. *Circulation* **124,** e906–e912 (2011).

8. Cines, D. B. *et al.* Endothelial Cells in Physiology and in the Pathophysiology of Vascular Disorders. *Blood* **91,** 3527–3561 (1998).

9. Rubanyi, G. M. The role of endothelium in cardiovascular homeostasis and diseases. *J. Cardiovasc. Pharmacol.* **22 Suppl 4,** S1-14 (1993).

10. Michiels, C. Endothelial cell functions. *J. Cell. Physiol.* **196,** 430–443 (2003).

11. Pober, J. S. & Sessa, W. C. Evolving functions of endothelial cells in inflammation. *Nat Rev Immunol* **7,** 803–815 (2007).

12. Libby, P. Inflammatory Mechanisms: the Molecular Basis of Inflammation and Disease. *Nutrition Reviews* **65,** S140–S146 (2007).

13. Komarova, Y. & Malik, A. B. Regulation of endothelial permeability via paracellular and transcellular transport pathways. *Annu. Rev. Physiol.* **72,** 463–493 (2010).

14. Kumar, P. *et al.* Molecular mechanisms of endothelial hyperpermeability: implications in inflammation. *Expert Rev Mol Med* **11,** e19 (2009).

15. Mehta, D. & Malik, A. B. Signaling Mechanisms Regulating Endothelial Permeability. *Physiological Reviews* **86,** 279–367 (2006).

16. Goddard, L. M. & Iruela-Arispe, M. L. Cellular and molecular regulation of vascular permeability. *Thromb Haemost* **109,** 407–415 (2013).

17. Sukriti, S., Tauseef, M., Yazbeck, P. & Mehta, D. Mechanisms regulating endothelial permeability. *Pulm Circ* **4,** 535–551 (2014).

18. Aghajanian, A., Wittchen, E. S., Allingham, M. J., Garrett, T. A. & Burridge, K. Endothelial cell junctions and the regulation of vascular permeability and leukocyte transmigration. *J Thromb Haemost* **6,** 1453–1460 (2008).

19. Chiu, J.-J. & Chien, S. Effects of Disturbed Flow on Vascular Endothelium: Pathophysiological Basis and Clinical Perspectives. *Physiological Reviews* **91,** 327–387 (2011).

20. Libby, P., Ridker, P. M. & Maseri, A. Inflammation and Atherosclerosis. *Circulation* **105,** 1135–1143 (2002).

21. Tedgui, A. & Mallat, Z. Anti-Inflammatory Mechanisms in the Vascular Wall. *Circulation Research* **88,** 877–887 (2001).

22. Xiao, L., Liu, Y. & Wang, N. New paradigms in inflammatory signaling in vascular endothelial cells. *AJP: Heart and Circulatory Physiology* **306,** H317–H325 (2014).

23. Zhou, J., Li, Y.-S. & Chien, S. Shear Stress–Initiated Signaling and Its Regulation of Endothelial Function. *Arterioscler Thromb Vasc Biol* ATVBAHA.114.303422 (2014). doi:10.1161/ATVBAHA.114.303422

24. Zhou, J., Li, Y.-S. & Chien, S. Shear Stress–Initiated Signaling and Its Regulation of Endothelial Function. *Arterioscler Thromb Vasc Biol* ATVBAHA.114.303422 (2014). doi:10.1161/ATVBAHA.114.303422

25. Cines, D. B. *et al.* Endothelial Cells in Physiology and in the Pathophysiology of Vascular Disorders. *Blood* **91,** 3527–3561 (1998).

26. Deanfield, J. E., Halcox, J. P. & Rabelink, T. J. Endothelial Function and Dysfunction Testing and Clinical Relevance. *Circulation* **115,** 1285–1295 (2007).

27. Libby, P. Inflammation in Atherosclerosis. *Arteriosclerosis, Thrombosis, and Vascular Biology* **32,** 2045–2051 (2012).

28. Danese, S., Dejana, E. & Fiocchi, C. Immune regulation by microvascular endothelial cells: directing innate and adaptive immunity, coagulation, and inflammation. *J. Immunol.* **178,** 6017–6022 (2007).

29. Lemichez, E., Lecuit, M., Nassif, X. & Bourdoulous, S. Breaking the wall: targeting of the endothelium by pathogenic bacteria. *Nat. Rev. Microbiol.* **8,** 93–104 (2010).

30. Methe, H., Hess, S. & Edelman, E. R. Endothelial immunogenicity--a matter of matrix microarchitecture. *Thromb. Haemost.* **98,** 278–282 (2007).

31. Mogensen, T. H. Pathogen recognition and inflammatory signaling in innate immune defenses. *Clin. Microbiol. Rev.* **22,** 240–273, Table of Contents (2009).

32. Peters, K., Unger, R. E., Brunner, J. & Kirkpatrick, C. J. Molecular basis of endothelial dysfunction in sepsis. *Cardiovascular Research* **60,** 49–57 (2003).

33. Newton, K. & Dixit, V. M. Signaling in Innate Immunity and Inflammation. *Cold Spring Harb Perspect Biol* **4,** a006049 (2012).

34. Opitz, B., Hippenstiel, S., Eitel, J. & Suttorp, N. Extra- and intracellular innate immune recognition in endothelial cells. *Thromb. Haemost.* **98,** 319–326 (2007).

35. Moser, M. *et al.* BMPER, a Novel Endothelial Cell Precursor-Derived Protein, Antagonizes Bone Morphogenetic Protein Signaling and Endothelial Cell Differentiation. *Mol. Cell. Biol.* **23,** 5664–5679 (2003).

36. Fiebig, J. E. *et al.* The clip-segment of the von Willebrand domain 1 of the BMP modulator protein Crossveinless 2 is preformed. *Molecules* **18,** 11658–11682 (2013).

37. Qiu, L., Zhang, J., Kotzsch, A., Sebald, W. & Mueller, T. D. Crystallization and preliminary X-ray analysis of the complex of the first von Willebrand type C domain bound to bone morphogenetic protein 2. *Acta Crystallogr. Sect. F Struct. Biol. Cryst. Commun.* **64,** 307–312 (2008).

38. Zhang, J.-L., Huang, Y., Qiu, L.-Y., Nickel, J. & Sebald, W. von Willebrand factor type C domain-containing proteins regulate bone morphogenetic protein signaling through different recognition mechanisms. *J. Biol. Chem.* **282,** 20002–20014 (2007).

39. Ikeya, M. *et al.* Essential pro-Bmp roles of crossveinless 2 in mouse organogenesis. *Development* **133,** 4463–4473 (2006).

40. Moser, M., Yu, Q., Bode, C., Xiong, J.-W. & Patterson, C. BMPER is a conserved regulator of hematopoietic and vascular development in zebrafish. *Journal of Molecular and Cellular Cardiology* **43,** 243–253 (2007).

41. Jo, H., Song, H. & Mowbray, A. Role of NADPH Oxidases in Disturbed Flow- and BMP4- Induced Inflammation and Atherosclerosis. *Antioxidants & Redox Signaling* **8,** 1609–1619 (2006).

42. Kelley, R. *et al.* A concentration-dependent endocytic trap and sink mechanism converts Bmper from an activator to an inhibitor of Bmp signaling. *J Cell Biol* **184,** 597–609 (2009).

43. Pi, X. *et al.* Bmper Inhibits Endothelial Expression of Inflammatory Adhesion Molecules and Protects Against Atherosclerosis. *Arterioscler Thromb Vasc Biol* **32,** 2214–2222 (2012).

44. Sorescu, G. P. *et al.* Bone Morphogenic Protein 4 Produced in Endothelial Cells by Oscillatory Shear Stress Induces Monocyte Adhesion by Stimulating Reactive Oxygen Species Production From a Nox1-Based NADPH Oxidase. *Circulation Research* **95,** 773–779 (2004).

45. Sucosky, P., Balachandran, K., Elhammali, A., Jo, H. & Yoganathan, A. P. Altered Shear Stress Stimulates Upregulation of Endothelial VCAM-1 and ICAM-1 in a BMP-4– and TGF-β1–Dependent Pathway. *Arterioscler Thromb Vasc Biol* **29,** 254–260 (2009).

46. Patel, N. *et al.* BMPER protein is a negative regulator of hepcidin and is up-regulated in hypotransferrinemic mice. *J. Biol. Chem.* **287,** 4099–4106 (2012).

47. Moreno-Miralles, I., Ren, R., Moser, M., Hartnett, M. E. & Patterson, C. Bone Morphogenetic Protein Endothelial Cell Precursor-Derived Regulator Regulates Retinal Angiogenesis In Vivo in a Mouse Model of Oxygen-Induced Retinopathy. *Arteriosclerosis, Thrombosis, and Vascular Biology* **31,** 2216–2222 (2011).

48. Helbing, T. *et al.* Krüppel-like factor 15 regulates BMPER in endothelial cells. *Cardiovasc. Res.* **85,** 551–559 (2010).

49. Helbing, T. *et al.* BMP activity controlled by BMPER regulates the proinflammatory phenotype of endothelium. *Blood* **118,** 5040–5049 (2011).

50. Helbing, T. *et al.* BMPER Is Upregulated by Statins and Modulates Endothelial Inflammation by Intercellular Adhesion Molecule–1. *Arterioscler Thromb Vasc Biol* **30,** 554–560 (2010).

51. Heinke, J. *et al.* BMPER is an endothelial cell regulator and controls bone morphogenetic protein-4-dependent angiogenesis. *Circ. Res.* **103,** 804–812 (2008).

52. Dyer, L., Wu, Y., Moser, M. & Patterson, C. BMPER-induced BMP signaling promotes coronary artery remodeling. *Dev. Biol.* **386,** 385–394 (2014).

53. Helbing, T. *et al.* Inhibition of BMP activity protects epithelial barrier function in lung injury. *J. Pathol.* **231,** 105–116 (2013).

54. Pi, X. *et al.* LRP1-dependent endocytic mechanism governs the signaling output of the bmp system in endothelial cells and in angiogenesis. *Circ. Res.* **111,** 564–574 (2012).

55. Surapisitchat, J. *et al.* Fluid shear stress inhibits TNF-α activation of JNK but not ERK1/2 or p38 in human umbilical vein endothelial cells: Inhibitory crosstalk among MAPK family members. *PNAS* **98,** 6476–6481 (2001).

56. Traub, O. & Berk, B. C. Laminar Shear Stress. *Arteriosclerosis, Thrombosis, and Vascular Biology* **18,** 677–685 (1998).

57. Berk, B. C. *et al.* Atheroprotective Mechanisms Activated by Fluid Shear Stress in Endothelial Cells. *Drug News Perspect.* **15,** 133–139 (2002).

58. Ku, D. N., Giddens, D. P., Zarins, C. K. & Glagov, S. Pulsatile flow and atherosclerosis in the human carotid bifurcation. Positive correlation between plaque location and low oscillating shear stress. *Arteriosclerosis, Thrombosis, and Vascular Biology* **5,** 293–302 (1985).

59. Asakura, T. & Karino, T. Flow patterns and spatial distribution of atherosclerotic lesions in human coronary arteries. *Circulation Research* **66,** 1045–1066 (1990).

60. Moore, J. E., Xu, C., Glagov, S., Zarins, C. K. & Ku, D. N. Fluid wall shear stress measurements in a model of the human abdominal aorta: oscillatory behavior and relationship to atherosclerosis. *Atherosclerosis* **110,** 225–240 (1994).

61. Chang, K. *et al.* Bone Morphogenic Protein Antagonists Are Coexpressed With Bone Morphogenic Protein 4 in Endothelial Cells Exposed to Unstable Flow In Vitro in Mouse Aortas and in Human Coronary Arteries Role of Bone Morphogenic Protein Antagonists in Inflammation and Atherosclerosis. *Circulation* **116,** 1258–1266 (2007).

62. Yao, Y. *et al.* Inhibition of Bone Morphogenetic Proteins Protects Against Atherosclerosis and Vascular Calcification. *Circulation Research* **107,** 485–494 (2010).

63. Derwall, M. *et al.* Inhibition of Bone Morphogenetic Protein Signaling Reduces Vascular Calcification and Atherosclerosis. *Arteriosclerosis, Thrombosis, and Vascular Biology* **32,** 613–622 (2012).

64. Moreno-Miralles, I., Schisler, J. C. & Patterson, C. New insights into bone morphogenetic protein signaling: focus on angiogenesis. *Curr Opin Hematol* **16,** 195–201 (2009).

65. Moser, M. & Patterson, C. Bone morphogenetic proteins and vascular differentiation: BMPing up vasculogenesis. *Thromb. Haemost.* **94,** 713–718 (2005).

66. Pi, X. *et al.* Sequential roles for myosin-X in BMP6-dependent filopodial extension, migration, and activation of BMP receptors. *J. Cell Biol.* **179,** 1569–1582 (2007).

67. Heinke, J. *et al.* Bone morphogenetic protein modulator BMPER is highly expressed in malignant tumors and controls invasive cell behavior. *Oncogene* **31,** 2919–2930 (2012).

68. Ren, R. *et al.* Gene expression profiles identify a role for cyclooxygenase 2-dependent prostanoid generation in BMP6-induced angiogenic responses. *Blood* **109,** 2847–2853 (2007).

69. Perez, V. A. de J. *et al.* BMP promotes motility and represses growth of smooth muscle cells by activation of tandem Wnt pathways. *J. Cell Biol.* **192,** 171–188 (2011).

70. Hong, J. H. *et al.* Effect of bone morphogenetic protein-6 on macrophages. *Immunology* **128,** e442-450 (2009).

71. Martin, G. S., Mannino, D. M., Eaton, S. & Moss, M. The Epidemiology of Sepsis in the United States from 1979 through 2000. *New England Journal of Medicine* **348,** 1546–1554 (2003).

72. Angus, D. C. & van der Poll, T. Severe Sepsis and Septic Shock. *New England Journal of Medicine* **369,** 840–851 (2013).

73. Mayr, F. B., Yende, S. & Angus, D. C. Epidemiology of severe sepsis. *Virulence* **5,** 4–11 (2014).

74. Andreakos, E. *et al.* Distinct pathways of LPS-induced NF-kappa B activation and cytokine production in human myeloid and nonmyeloid cells defined by selective utilization of MyD88 and Mal/TIRAP. *Blood* **103,** 2229–2237 (2004).

75. Kisseleva, T. *et al.* NF-κB regulation of endothelial cell function during LPS-induced toxemia and cancer. *J Clin Invest* **116,** 2955–2963 (2006).

76. Gandhirajan, R. K. *et al.* Blockade of NOX2 and STIM1 signaling limits lipopolysaccharide-induced vascular inflammation. *J. Clin. Invest.* **123,** 887–902 (2013).

77. Zanoni, I. *et al.* CD14 regulates the dendritic cell life cycle after LPS exposure through NFAT activation. *Nature* **460,** 264–268 (2009).

78. Hijiya, N. *et al.* Possible involvement of toll-like receptor 4 in endothelial cell activation of larger vessels in response to lipopolysaccharide. *Pathobiology* **70,** 18–25 (2002).

79. Dyer, L. A., Pi, X. & Patterson, C. The role of BMPs in endothelial cell function and dysfunction. *Trends Endocrinol. Metab.* (2014). doi:10.1016/j.tem.2014.05.003

80. Bacskai, B. J., Xia, M. Q., Strickland, D. K., Rebeck, G. W. & Hyman, B. T. The endocytic receptor protein LRP also mediates neuronal calcium signaling via N-methyl-d-aspartate receptors. *PNAS* **97,** 11551–11556 (2000).

81. Hayashi, H., Campenot, R. B., Vance, D. E. & Vance, J. E. Apolipoprotein E-Containing Lipoproteins Protect Neurons from Apoptosis via a Signaling Pathway Involving Low-Density Lipoprotein Receptor-Related Protein-1. *J. Neurosci.* **27,** 1933–1941 (2007).

82. Hu, K. *et al.* Tissue-type Plasminogen Activator Acts as a Cytokine That Triggers Intracellular Signal Transduction and Induces Matrix Metalloproteinase-9 Gene Expression. *J. Biol. Chem.* **281,** 2120–2127 (2006).

83. Mantuano, E. *et al.* The hemopexin domain of matrix metalloproteinase-9 activates cell-signaling and promotes migration of Schwann cells by binding to low density lipoprotein receptor-related protein. *J Neurosci* **28,** (2008).

84. Mantuano, E., Mukandala, G., Li, X., Campana, W. M. & Gonias, S. L. Molecular Dissection of the Human α2-Macroglobulin Subunit Reveals Domains with Antagonistic Activities in Cell Signaling. *J. Biol. Chem.* **283,** 19904–19911 (2008).

85. Boucher, P. & Herz, J. Signaling through LRP1: Protection from atherosclerosis and beyond. *Biochem. Pharmacol.* **81,** 1–5 (2011).

86. Geer, P. van der. Phosphorylation of LRP1. *Trends in Cardiovascular Medicine* **12,** 160–165 (2002).

87. Mao, H., Lockyer, P., Townley-Tilson, W. H. D., Xie, L. & Pi, X. LRP1 Regulates Retinal Angiogenesis by Inhibiting PARP-1 Activity and Endothelial Cell Proliferation. *Arteriosclerosis, Thrombosis, and Vascular Biology* **36,** 350–360 (2016).

88. Mao, H. *et al.* Endothelial LRP1 regulates metabolic responses by acting as a co-activator of PPARγ. *Nature Communications* **8,** ncomms14960 (2017).

89. Jennings, C., Kusler, B. & Jones, P. P. Calcineurin inactivation leads to decreased responsiveness to LPS in macrophages and dendritic cells and protects against LPS-induced toxicity in vivo. *Innate Immun* **15,** 109–120 (2009).

90. Obasanjo-Blackshire, K. *et al.* Calcineurin regulates NFAT-dependent iNOS expression and protection of cardiomyocytes: co-operation with Src tyrosine kinase. *Cardiovasc. Res.* **71,** 672–683 (2006).

91. Li, Y., van Kerkhof, P., Marzolo, M. P., Strous, G. J. & Bu, G. Identification of a Major Cyclic AMP-Dependent Protein Kinase A Phosphorylation Site within the Cytoplasmic Tail of the Low-Density Lipoprotein Receptor-Related Protein: Implication for Receptor-Mediated Endocytosis. *Mol Cell Biol* **21,** 1185–1195 (2001).

92. Rooney, J. W., Sun, Y. L., Glimcher, L. H. & Hoey, T. Novel NFAT sites that mediate activation of the interleukin-2 promoter in response to T-cell receptor stimulation. *Mol. Cell. Biol.* **15,** 6299–6310 (1995).

93. Himes, S. R., Coles, L. S., Reeves, R. & Shannon, M. F. High Mobility Group Protein I(Y) Is Required for Function and for c-Rel Binding to CD28 Response Elements within the GM-CSF and IL-2 Promoters. *Immunity* **5,** 479–489 (1996).

94. May, P., Reddy, Y. K. & Herz, J. Proteolytic Processing of Low Density Lipoprotein Receptor-related Protein Mediates Regulated Release of Its Intracellular Domain. *J. Biol. Chem.* **277,** 18736–18743 (2002).

95. Shamanna, R. A. *et al.* The NF90/NF45 Complex Participates in DNA Break Repair via Nonhomologous End Joining ▽. *Mol Cell Biol* **31,** 4832–4843 (2011).

96. Karmakar, S., Mahajan, M. C., Schulz, V., Boyapaty, G. & Weissman, S. M. A multiprotein complex necessary for both transcription and DNA replication at the β-globin locus. *EMBO J* **29,** 3260–3271 (2010).

97. Reichman, T. W., Muñiz, L. C. & Mathews, M. B. The RNA Binding Protein Nuclear Factor 90 Functions as Both a Positive and Negative Regulator of Gene Expression in Mammalian Cells. *Mol Cell Biol* **22,** 343–356 (2002).

98. Sakamoto, S. *et al.* The NF90-NF45 Complex Functions as a Negative Regulator in the MicroRNA Processing Pathway. *Mol Cell Biol* **29,** 3754–3769 (2009).

99. Guan, D. *et al.* Nuclear Factor 45 (NF45) Is a Regulatory Subunit of Complexes with NF90/110 Involved in Mitotic Control. *Mol Cell Biol* **28,** 4629–4641 (2008).

100. Zhao, G., Shi, L., Qiu, D., Hu, H. & Kao, P. N. NF45/ILF2 tissue expression, promoter analysis, and interleukin-2 transactivating function. *Exp. Cell Res.* **305,** 312–323 (2005).

101. Nirula, A., Moore, D. J. & Gaynor, R. B. Constitutive Binding of the Transcription Factor Interleukin-2 (IL-2) Enhancer Binding Factor to the IL-2 Promoter. *J. Biol. Chem.* **272,** 7736–7745 (1997).

102. Ambrosio, A. L. *et al.* Crossveinless-2 Is a BMP Feedback Inhibitor that Binds Chordin/BMP to Regulate Xenopus Embryonic Patterning. *Developmental Cell* **15,** 248–260 (2008).

103. Coles, E., Christiansen, J., Economou, A., Bronner-Fraser, M. & Wilkinson, D. G. A vertebrate crossveinless 2 homologue modulates BMP activity and neural crest cell migration. *Development* **131,** 5309–5317 (2004).

104. Conley, C. A. *et al.* Crossveinless 2 contains cysteine-rich domains and is required for high levels of BMP-like activity during the formation of the cross veins in Drosophila. *Development* **127,** 3947–3959 (2000).

105. Ikeya, M. *et al.* Cv2, functioning as a pro-BMP factor via twisted gastrulation, is required for early development of nephron precursors. *Developmental Biology* **337,** 405–414 (2010).

106. Ikeya, M. *et al.* Essential pro-Bmp roles of crossveinless 2 in mouse organogenesis. *Development* **133,** 4463–4473 (2006).

107. Kamimura, M., Matsumoto, K., Koshiba-Takeuchi, K. & Ogura, T. Vertebrate crossveinless 2 is secreted and acts as an extracellular modulator of the BMP signaling cascade. *Dev. Dyn.* **230,** 434–445 (2004).

108. Rentzsch, F., Zhang, J., Kramer, C., Sebald, W. & Hammerschmidt, M. Crossveinless 2 is an essential positive feedback regulator of Bmp signaling during zebrafish gastrulation. *Development* **133,** 801–811 (2006).

109. Serpe, M. *et al.* The BMP-Binding Protein Crossveinless 2 Is a Short-Range, Concentration-Dependent, Biphasic Modulator of BMP Signaling in Drosophila. *Developmental Cell* **14,** 940–953 (2008).

110. Shi, Y., Mantuano, E., Inoue, G., Campana, W. M. & Gonias, S. L. Ligand Binding to LRP1 Transactivates Trk Receptors by a Src Family Kinase–Dependent Pathway. *Sci. Signal.* **2,** ra18-ra18 (2009).

111. Matute-Bello, G. *et al.* Fas (CD95) Induces Alveolar Epithelial Cell Apoptosis in Vivo. *Am J Pathol* **158,** 153–161 (2001).

112. Itoh, T. *et al.* Adrenomedullin ameliorates lipopolysaccharide-induced acute lung injury in rats. *American Journal of Physiology - Lung Cellular and Molecular Physiology* **293,** L446–L452 (2007).

113. Ronnebaum, S. M., Wu, Y., McDonough, H. & Patterson, C. The Ubiquitin Ligase CHIP Prevents SirT6 Degradation through Noncanonical Ubiquitination. *Mol. Cell. Biol.* **33,** 4461–4472 (2013).